Journal of CO2 Utilization 83 (2024) 102825

Contents lists available at ScienceDirect

Journal of CO2 Utilization

journal homepage: www.elsevier.com/locate/jcou

Benchmarking microwave-induced CO_2 plasma splitting against electrochemical CO_2 reduction for a comparison of promising technologies

A. Hecimovic [a,*], M.T. Mayer [b,*], L.G.J. de Haart [c,*], S. Gupta [b], C.K. Kiefer [a], A. Navarrete [d], A. Schulz [e], U. Fantz [a]

[a] Max-Planck-Institut für Plasmaphysik, Germany
[b] Helmholtz-Zentrum Berlin für Materialien und Energie, Germany
[c] Institute of Energy and Climate Research, Fundamental Electrochemistry (IEK-9), Forschungszentrum Jülich GmbH, Germany
[d] Institute for Micro Process Engineering (IMVT), Karlsruhe Institute of Technology (KIT), Germany
[e] University of Stuttgart, Institute of Interfacial Process Engineering and Plasma Technology (IGVP), Germany

ARTICLE INFO

Keywords:
CO2 conversion
CO2 high temperature electrolysis
CO2 low temperature electrolysis
CO2 microwave plasma conversion
Technical comparison

ABSTRACT

Plasma conversion technology is an emerging technique under development to activate, convert or valorize gas molecules such as CO_2, N_2, CH_4, NH_3 and others. A large-scale application beyond the lab-scale demonstrator unit requires assessment of the efficiency of this new technology. The straightforward approach for assessment of the efficiency is benchmarking with the other well-established technologies of similar technology readiness level (TRL). In this paper we present a benchmarking of the atmospheric pressure microwave-induced CO_2 plasma splitting with electrochemical CO_2 conversion, via both low-temperature and high-temperature electrolysis. An additional step of oxygen removal in case of the plasma reactor is implemented due to the difference in the output stream of the plasma (gas mixture containing CO_2, CO, and O_2) and the electrochemical reactor (typical gas mixture on cathode containing CO_2 and CO). For the benchmarking, a comprehensive set of comparison parameters that are applicable for both the plasma and the electrochemical route is identified and grouped in three comparison categories: performance, interfaces, and economics. The comparison of these parameters demonstrates that in terms of the electric power consumption (EPC; power required for production of one Nm^3_{CO}) plasma conversion technology (~20 kWh/Nm^3_{CO}) is in the ballpark with the other two electrochemical technologies (~4–20 kWh/Nm^3_{CO}). The key features of the plasma conversion technology are relatively large conversion (up to 56%) and moderate energy efficiencies (up to 27%). Also, CO_2 gas of reduced purity of only 98% can be used without decrease of the performance, and CO output values are currently at 3.5 slm (standard litre per minute). Fast on/off response time of order of minutes, and no need for the hot standby indicate that the plasma conversion is particularly suitable for use of intermittent renewable energy sources. The aspects that require further development include optimization of the process towards lower EPC_{total} values, improved oxygen gas separation, and reliable ignition of the plasma.

1. Introduction

Development of new CO_2 conversion and utilization technologies is one of the key strategies to help reduce both CO_2 concentration in the atmosphere and CO_2 emissions, in order to mitigate global warming caused by enhanced greenhouse gas concentrations in the Earth's atmosphere [1]. The new technologies should preferably be only electricity driven in order to be compatible with renewable electricity sources (solar, wind, etc.), either operated continuously or intermittently, particularly when the renewable electricity production cannot be distributed in the electricity network, via so-called peak shaving [2]. In that sense, plasma conversion technology and both low- and high- temperature electrolysis are compatible with renewable energy sources.

While CO_2 can be converted into a variety of value-added products (including hydrocarbons, alcohols, aldehydes, and organic acids, [3]), carbon monoxide (CO) is a particularly interesting product for several reasons. When using electrolysis, CO is one of the simplest products

* Corresponding authors.
E-mail addresses: ante.hecimovic@ipp.mpg.de (A. Hecimovic), m.mayer@helmholtz-berlin.de (M.T. Mayer), l.g.j.de.haart@fz-juelich.de (L.G.J. de Haart).

https://doi.org/10.1016/j.jcou.2024.102825
Received 21 March 2024; Received in revised form 8 May 2024; Accepted 25 May 2024
Available online 31 May 2024

formed from CO_2, requiring one CO_2 molecule and two electron transfers, meaning the selectivity and efficiency of the process can more readily be optimized compared to the more complex reaction products. CO is a high-volume commodity chemical in the chemical industry, utilized in synthesis gas (syngas) at about 598 Mt/y globally [4]. CO has many applications in bulk chemicals manufacturing, including combination with H_2 to form syngas for generating a range of synthetic fuels [5]. Presently, most industrial CO is produced by steam reforming of methane, which leads to significant emissions of CO_2 as byproduct [4,6]. Hence, new approaches to sustainable synthesis of carbon-neutral "green CO" are urgently required. For each of the emerging approaches discussed herein (plasma conversion, low and high temperature CO_2 electrolysis), the systems for CO_2 conversion closest to commercialization are the ones producing CO, which are therefore the basis of comparison in this article.

Plasma conversion technology is investigated as a potential technology for conversion of gases, aiming at optimizing the efficiency of the process in order to replace current energy-intensive technologies [7]. The basis of a plasma process for gas conversion is the delivery of energy to the free electrons (typically by applying an electric field in which the electrons are accelerated) which through elastic and inelastic collision transfer the energy to the atoms and molecules. In short, the plasma can fulfil two basic roles: if suitable non-equilibrium conditions can be achieved as means to facilitate reaction pathways entirely inaccessible by purely thermal approaches by lowering the energy barrier through population of higher vibrational and rotational levels, or to serve as a supplier of heat (several 1000 K can easily be reached, depending on the discharge type). However, in most applications the plasma may act as both, which makes understanding its specific function in the process chemistry a very complex and actively investigated topic [8–11]. The main challenges are optimization of the conversion and the energy efficiency, particularly at atmospheric pressure as it is regarded more attractive for an industrial application of the plasma, and separation of oxygen from the plasma outflow towards achieving CO and CO_2 gas mixtures.

Electrochemical technologies involve the inter-conversion of electrical and chemical energy by charge transfer processes at a catalyst electrodes/electrolyte interface (e.g. water electrolysis for H_2 production, or releasing electrical power from H_2 and O_2 in fuel cells). Direct electrochemical conversion of CO_2 (CO_2 electrolysis) has been studied for several decades and has recently seen rapid scientific and technological progress [12–14]. A variety of electrochemical approaches to CO_2 conversion have been proposed, spanning a range of technology readiness levels (TRLs), with some examples reaching early-stage commercialization. Approaches to CO_2 electrolysis can be broken down into two general categories: low-temperature (near ambient) (LT electrolysis) and high-temperature electrolysis (HT electrolysis) [5]. Both involve a cathode (where CO_2 is electrochemically reduced), an anode (where something is oxidized to liberate electrons) and an electrolyte for the transport of ions. However, the two approaches differ in their operating principles and materials. Namely, the low-temperature approaches typically use ion-exchange membranes and/or liquid electrolytes for ion transport and operate at near room temperature, while high-temperature cells rely on solid oxide materials which conduct oxygen ions best at elevated temperatures.

Regarding low-temperature (LT) electrolyzers, present state-of-the-art device concepts resemble fuel cells or water electrolyzers, with gas diffusion electrodes facilitating transport of gas-phase reactants and products to enable industrially relevant reaction rates [15]. Much of the research focus has been on the central challenge of product selectivity, since upwards of 20 different CO_2-derived products can be formed as an undesirable mixture [16,17], in addition to H_2 evolution [16]. Only recently are more application-oriented metrics receiving significant attention, including stability, energy efficiency, and product purity. Nonetheless, there is recent progress towards CO production with high selectivity and high conversion yield in scalable devices [14,18,19].

Already in the 1980s the investigation of high temperature (HT) electrolysis of steam and carbon dioxide gained interest [20]. In the framework of the so called "HOT-ELLY" project the German company Dornier worked on the development of large-scale hydrogen production using high-temperature steam electrolysis [21–24]. With the end of the project the research on high-temperature steam electrolysis remained quiet for almost two decades. Starting in the same decade, and continuously thereafter, NASA and associated partners investigated the high temperature electrolysis of carbon dioxide for oxygen production in view of manned space missions to Mars [25–27]. Riding with the Perseverance rover during NASA's Mars mission in recent years, oxygen production from carbon dioxide was successfully demonstrated with the Mars Oxygen In-Situ Resource Utilization Experiment (MOXIE) technology demonstrator employing HT electrolysis [28].

The research and development of these Solid Oxide Electrolysis Cells (SOEC) with oxygen ion-conducting ceramic electrolytes is closely related to the development of Solid Oxide Fuel Cell (SOFC), which has gone through an impressive progress in the last decades. This, together with the aforementioned drive for renewable energy conversion technologies, renewed the interest in high temperature electrolysis in the past years. Not only for steam [29–31] and for carbon dioxide electrolysis [5,12,13,30,32–34] but also for mixtures of steam and carbon dioxide, the so-called co-electrolysis [35–38], to produce syngas. Most of the research is concentrated on improvement of the power density and the durability of the cells and other stack components. This includes amongst others the development of new electrocatalytic active materials specific to either the steam or carbon dioxide reduction reaction or the oxygen evolution reaction. Already in 2017, the Danish company Haldor Topsøe A/S (HTAS) introduced the first commercial HT CO_2 electrolysis system, although at the time with a small-scale production capacity up to 10 Nm^3 CO_2 per hour [39].

In this paper the present-day performance of three technologies for electrically-driven CO_2 conversion to CO is compared at both lab-scale and industrial-scale: plasma conversion technology, LT electrolysis, and HT electrolysis. The comparison considers three aspects: 1) production and efficiency, 2) requirements regarding the interfaces, and 3) economic considerations.

2. CO_2 conversion technologies

In this section fundamental aspects of the plasma conversion technology, as well LT electrolysis and HT electrolysis are presented.

2.1. Plasma conversion technology

Plasma based gas conversion is an emerging technology that is capable of activating stable molecules such as CH_4, CO_2, N_2 or H_2O by efficiently breaking their chemical bonds and converting them into value-added chemicals. The choice of discharge and operating pressure allows to tune the plasma properties and optimize the gas dissociation [40]. One of the most promising type of the plasma for CO_2 dissociation in pressure range 200–1000 mbar is the microwave plasma due to high flexibility, and higher conversion and energy efficiencies obtained compared to other types of discharges [9–11,40]. Recently, high conversions at atmospheric pressure are demonstrated when quenching the gas temperature in the plasma effluent by either using a water-cooled nozzle or water-cooled channels [41,42]. Furthermore, measurements of the industrially relevant parameters, such as wall plug efficiency, durability and impact of impurities were performed demonstrating suitability of the plasma for dynamic intermittent operation, and insensitivity to impurities in the inlet gas stream up to about 2% [43].

In this work a microwave (MW) plasma reactor (microwave plasma torch [44,45]) is used for benchmarking CO production from CO_2, operating at atmospheric pressure in order to make it comparable with the electrolyzer reactors. Two variations of the microwave torch are used, as shown in Fig. 1. One configuration is used as an example of a

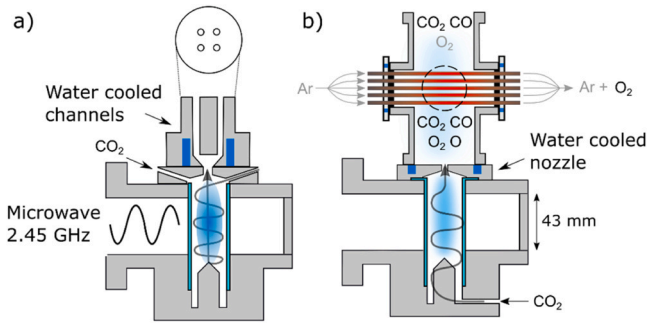

Fig. 1. Schematic representation of the atmospheric pressure microwave plasma torch with a) four cooled effluent channels (cross section of the channels is shown above the schematic), and b) nozzle and oxygen separation membranes. Microwave power levels up to 3 kW, and CO_2 flows in the range 3.7–20 slm are used.

plasma reactor with the highest conversion currently achievable at atmospheric pressure, which is obtained using the cooled effluent channels and a reverse vortex as shown in Fig. 1a) (referred to "MW plasma reactor" in the following). The other experiment with a nozzle shown in Fig. 1b) is an example of plasma reactor with relatively high conversion for which the additional oxygen separation step is added (referred to "MW plasma reactor with membranes" in the following). The reasoning for using the configuration with the nozzle will be explained in the following paragraphs.

The difference in the performance of the two plasma torch geometries stems from the way the gas in the plasma effluent is cooled. In both configurations the CO_2 gas is confined inside the quartz tube which is placed inside the 2.45 GHz microwave resonator where the plasma is ignited. At atmospheric pressure the CO_2 plasma is confined to the center of the quartz tube reaching temperatures of 6000 °C [11,46], with some portion of the CO_2 gas swirling around the plasma. This high temperature of the CO_2 gas indicates that the thermal dissociation is strongly contributing to the total conversion. Fast cooling (quenching) of the gas in the plasma effluent with about 10^7 K/s is very important in order to prevent the recombination of the dissociated CO into CO_2 [8]. In the configuration with the cooled effluent channels and the reverse vortex the gas is introduced tangentially at the top of the resonator swirling down along the walls of the quartz tube and streaming upward through the plasma region. In this configuration the cooling of the gas in the plasma effluent is achieved via convective gas-surface cooling inside the cooling channels. The gas temperature behind the cooled channels is in the range 300–400 °C, which is too low to activate the oxygen separation membranes. In the configuration with the nozzle the gas is introduced tangentially at the bottom of the resonator swirling upwards. Here, the cooling of the gas in the plasma effluent is achieved by enhancing the gas mixing inside the nozzle (the gas is mixed by passing through a nozzle, effectively quenching the temperature of the gas that has passed through the plasma) and by conductive cooling through contact with the cooled nozzle surface. In the configuration with the nozzle (Fig. 1b) the temperature behind the nozzle is about 1000 °C which is high enough to activate oxygen separation membranes and low enough to prevent recombination.

Different from the electrolysis processes wherein the main products of the CO_2 decomposition are separated on the anode (O_2) and on the cathode (CO) (more details in Sections 2.2 and 2.3), in the MW plasma reactor the CO_2 dissociation products remain unseparated. Therefore, for a direct comparison of the plasma conversion process outflow, an oxygen separation step is required, which is included in the detailed analysis. For many applications of the CO gas (e.g. Fischer-Tropsch fuel synthesis) oxygen concentration is tolerated only in small quantities up to maximum 1% [47]. O_2 removal in the plasma effluent has been attempted either by using a nanostructured CeO_2/Fe_2O_3 oxygen scavenger [48], oxygen permeable membranes [49,50], a carbon bed [51], or by a coupled plasma-electrolysis process [52] with limited success. So far, an efficient way to remove large amounts of oxygen (reaching below 1% concentration) in a continuous way has not been found.

Gas temperatures in the plasma effluent of about 1000 °C are envisaged since they are required to activate the perovskite membranes used for the oxygen separation step. As shown in Fig. 1b) the membranes are mounted in the plasma effluent at the distance where the gas temperature is in the range 800–1200 °C, with Ar gas sweeping through the membranes and removing oxygen that permeated to the inside of the LCCF membranes [53]. A demonstrator setup with nozzle and 21 membranes is investigated. The amount of oxygen separated is still rather low at 42 sccm (standard cubic centimeter), which is 5% of the produced oxygen flow. Nevertheless, it is a demonstration of the capability to thermally activate multiple LCCF membranes for oxygen permeation by placing them in the effluent of a CO_2 plasma.

The performance of the plasma source is assessed by measuring the CO_2 conversion of the gas stream that passed the plasma. The enthalpy of the CO_2 dissociation process is:

$$CO_2 \rightarrow CO + \frac{1}{2}O_2, \quad \Delta H = 2.93eV \Big/ molecule \tag{1}$$

in a two-step process, dissociation of the CO_2 molecule by breaking of the C-O bond which requires a minimum energy of 5.5 eV, and subsequent formation of the O_2 molecule in interaction between a vibrationally excited CO_2* molecule and the oxygen atom:

$$CO_2 \rightarrow CO + O, \quad \Delta H = 5.5eV/molecule \tag{2}$$

$$CO_2^* + O \rightarrow CO + O_2, \quad \Delta H = 0.3eV/molecule \tag{3}$$

In Eq. (3), the enthalpy calculation is done for a CO_2 molecule in a ground state, whereas the vibrational energy of the CO_2 molecule contributes to the reaction enthalpy. According to the literature activation energy of the reaction is between 0.5–1 eV/molecule [8]. Measurement of the gas composition downstream of the plasma by a mass spectrometer [54] allows to calculate the CO_2 conversion using the measured relative molar flows of CO_2 ($\dot{n}_{CO_2,out}$) and sum of the molar flows of CO_2, CO, O_2, ($\dot{n}_{total,out}$) using the following equation:

$$\chi_{CO_2} = \frac{1 - \frac{\dot{n}_{CO_2,out}}{\dot{n}_{total,out}}}{1 + \frac{\dot{n}_{CO_2,out}}{2\dot{n}_{total,out}}} \tag{4}$$

which is correlated with the commonly used equation $\chi_{CO_2} = 1 - \frac{\dot{n}_{CO_2,out}}{\dot{n}_{CO_2,in}}$ under the assumption of stoichiometric CO_2 dissociation into CO and ½ O_2. Other ways to calculate the CO_2 conversion can be found elsewhere [55]. It is important to mention that in the MW plasma reactor no carbon deposits are observed and stoichiometry of the reaction is preserved. The plasma energy efficiency η is calculated from:

$$\eta = \chi_{CO_2} \frac{\Delta H}{SEI} \tag{5}$$

whereby ΔH is the enthalpy of CO_2 dissociation as described above (2.93 eV/molecule), and specific energy input (SEI) is calculated as a ratio of the power deposited in the plasma P_p divided by the inflow rate of CO_2 gas (SEI [eV/molecule] = 0.0139 *P_p[W]/$flow_{CO2}$[slm]). The gas flow rate in slm is quantified in standard liters per minute (slm).

2.1.1. Interfaces

The interfaces of the plasma conversion process comprise the properties of the CO_2 gas (e.g. purity, pressure) at the inlet and properties of the product gases at the outlet, and power required to operate the experiment. In order to integrate with the rest of the production chain, upscaling and automation aspects should also be addressed.

The purity of the CO_2 inlet gas influences the efficient operation of the MW plasma reactor. Most laboratory experiments are conducted on research-grade CO_2 (N3.5–4.0, i.e. $\geq$ 99.95 – 99.99%). A recent study demonstrated that plasma conversion is not sensitive to impurities in the inlet gas stream up to about 2% as long as this impurity is not water vapor that reduces the conversion strongly [43]. Above 2% of impurity concentration the CO_2 conversion typically decreases, and the reduction rate depends on the impurity gas. These values are in the range of the CO_2 purity coming from direct air capture sources [56,57].

The power delivered to the MW plasma reactor can be continuous or intermittent. The test performed in a recent study demonstrated that a MW plasma reactor can deliver very reproducible results in a test where plasma was operated over 6 days intermittently in steps ranging from 5 hours to 9 hours without interruption [43]. This performance demonstrated suitability of the plasma conversion technology for dynamic intermittent operation. It is possible to measure both the power deposited in the plasma P_p, allowing to calculate the energy efficiency of the plasma process (Eq. (5)), and the total power used by the plasma power supply and other peripheral devices P_{tot}. The measured total power is used to calculate the wall plug efficiency η_{tot} by using the following equation:

$$\eta_{tot} = \chi_{CO_2} \frac{\Delta H}{SEI_{tot}} \tag{6}$$

where SEI_{tot} is the specific energy input, calculated as a ratio of the total power consumed by the plasma power supply and all peripheral devices P_{tot} divided by the CO_2 gas flow rate (SEI [eV/molecule] = 0.0139 $*P_{tot}[W]/flow_{CO2}[slm]$).

The maximum power available from the microwave supply for the above described experiments is 3 kW. Using multiple MW plasma reactors with multiple sources placed in parallel is one option for increasing the power and CO output. Other options for upscaling the plasma technology are increasing the power of the 2.45 GHz microwave source, with 15 kW available as the highest power rated device [58], or changing the frequency of the microwave to 915 MHz [59]. Decrease in the frequency results in increase of the microwave waveguide size (proportional to the increase in microwave wavelength) that can accommodate larger quartz tubes (consequently larger CO_2 flows) with available power sources up to 100 kW [58,60]. However, it is yet to be demonstrated that the CO_2 conversion and the energy efficiency will scale with the power in either 2.45 GHz or 915 MHz microwave plasma sources.

Typically, operational pressure of the plasmas for gas conversion ranges from several mbar to atmospheric pressure. Sub-atmospheric pressure experiments are more suited for fundamental investigation of the gas dissociation pathways [10,61], while experiments at atmospheric pressure or above are suitable for both fundamental investigations and an effort towards industrial application of the technology [41,42]. An attempt to operate the gas conversion plasmas at pressures above atmospheric pressure has been reported only recently demonstrating an increase of the CO_2 conversion and efficiency with increased pressure for the investigated setup [62]. The experiments reported here are performed at atmospheric pressure for compatibility with the electrolysis experiments, thus delivering the CO containing gas mixture to the next step at atmospheric pressure.

In the MW plasma reactor an additional oxygen separation step is required since the CO_2 dissociation products remain unseparated in contrast to the electrolysis where the main products of the CO_2 decomposition are separated on the anode (O_2) and on the cathode (CO, CO_2). The experiment described in Section 2.1 is designed as a demonstrator reactor to show that it is possible to remove the oxygen using perovskite membranes heated by the hot gas in the plasma effluent. As mentioned earlier the amount of oxygen separated was still rather low at about 5% of the produced oxygen flow [53]. The O_2 separation step did not influence the CO production rate and the precise CO outflow is given for both experiments: MW plasma reactor and MW plasma reactor with membranes.

Ideally the plasma would be a turnkey process that is seamlessly integrated with the rest of the fuel or similar production chain. The MW plasma reactor presented in this paper uses a pin for ignition at atmospheric pressure [44,45], which is functioning as intended until sputtering and erosion affect the sharpness of the pin resulting in a reduced electric field strength at the tip, preventing ignition. A solution is to be found in future, e.g. using a material which is less prone to sputtering and erosion like tungsten.

2.1.2. Lab-scale experiments vs industrial-scale setups

The lab-scale experiments used for the comparison (Section 4) are described in this section. Two experiments will be used, one demonstrating the highest performance, and the other demonstrating high performance and an additional oxygen separation step. Both of these setups are a lab-scale experiments and are not yet optimised for an industrial application, therefore the TRL of these two plasma sources is estimated to be TRL 4 - Technology validated in lab. The current power supply delivers up to 3 kW of microwave power, and typically CO_2 inlet flow rates used are in range 3.7–20 slm. There is still ample space for improvement of these setups. For example, the most suitable power and CO_2 flow rate in terms of optimum CO_2 conversion and energy efficiency can be tuned, and subsequently a choice of an optimal power supply that has maximum efficiency at that chosen power can be made. The improved performance of the microwave plasma torch at a given CO_2 flow rate is achievable by adjusting the geometry of the cooling channels (number, length diameter) for maximum gas quenching. Finally, increase in the number of oxygen permeation membranes toward oxygen removal below 1% is required.

There are no known industrial-scale setups available for comparison of the plasma CO_2 conversion with the lab-scale experiment. Therefore, for the data concerning the industry-like application the setup assembled during the KEROGREEN project is used [63]. The setup consisted of a 915 MHz microwave plasma torch reactor, equipped with a 6 kW power supply, and CO_2 inlet flow rates up to 60 slm. As part of the project the MW plasma reactor was mounted inside a container used for production of green kerosene. Behind the MW plasma reactor, it was intended that the gas mixture goes into an electrochemically based oxygen separator and a pressure swing adsorption module to purify the gas stream [52]. The upscaling of the oxygen separation step consisting of a coupled plasma-electrolysis process is still to be successfully implemented [64]. Subsequently the CO is converted into kerosene by means of advanced sorption enhanced water gas shift and process-intensified Fischer-Tropsch synthesis followed by hydrocracking [64]. It is considered that integrating the plasma process in the complete cycle this technology to has reached TRL level 5 - Technology validated in relevant environment.

2.2. Low temperature electrolysis

Low temperature (LT) electrolysis refers to devices employing liquid electrolytes, ion-exchange membranes, or both, typically operating at mild temperatures between 20 °C and 100 °C. As depicted in Fig. 2, the core components are the cathode where electrochemical CO_2 reduction takes place, the anode where a complementary oxidation half-reaction occurs (usually O_2 evolution from water), the liquid electrolyte and/or ion exchange membrane (for transporting ions), and the external circuit which supplies electrical power. CO_2 (gas phase, humidified, or solvated) is provided to the cathode which is functionalized with electrocatalysts that facilitate multiple electron and proton transfer steps to form reduced products.

Production of carbon monoxide via two-electron reduction of CO_2 is represented in Eq. (7). When paired with water oxidation at the anode (Eq. (8)), the net cell reaction is Eq. (9).

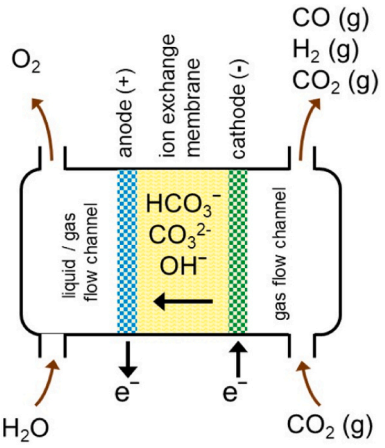

Fig. 2. General schematic representation of the LT electrolysis cell. Numerous cell configuration variations exist [15,65], involving combinations of liquid electrolyte in the anode and/or cathode channels (usually containing dissolved salt, e.g. KOH), separators (anion- or cation-exchange, bipolar membrane, porous frit), and cell geometries.

$$CO_2 + H_2O + 2e^- \rightarrow CO + 2OH^- \quad (7)$$

$$2OH^- \rightarrow H_2O + \frac{1}{2}O_2 + 2e^- \quad (8)$$

$$CO_2 \rightarrow CO + \frac{1}{2}O_2 \quad (9)$$

A prominent side reaction, which can occur at cathodes in aqueous environments, is the hydrogen evolution reaction (HER), Eq. (10). When pure CO streams are desired, the HER is considered parasitic, but when the goal is to directly generate syngas ($CO+H_2$ mixtures) by co-electrolysis of CO_2 and water, the reaction may be desirable.

$$2H_2O + 2e^- \rightarrow H_2 + 2OH^- \quad (10)$$

Besides carbon monoxide, it should be noted that LT electrolysis can directly generate a wide variety of other valuable products including multi-carbon oxygenates and hydrocarbons, which differentiates the technology from HT electrolysis and plasma approaches. However, product selectivity remains a great challenge when targeting higher-order products, since they are often produced as an undesirable mixture [17].

In a typical LT electrolysis cell, CO_2 gas flows through the cathode compartment, a negative bias potential is applied to the cathode to produce cathodic current, and products are generated at the electrochemical interface. Electrical currents are typically expressed as current densities (normalized to the electrode geometric area). Gas products such as CO are carried out of the cell for collection or on-line analysis (e.g. by gas chromatography). Commonly, the measured product generation rates are expressed as partial current densities ($J_{product}$), to facilitate comparison with the total measured current density (J_{tot}) for calculation of the faradaic efficiency (*FE*) toward a given product:

$$FE_{product} = \frac{J_{product}}{J_{tot}} \cdot 100\% \quad (11)$$

For instance, perfect CO selectivity would be represented by an FE_{CO} of 100%, meaning all charge went toward generating the product of interest.

It should be noted that product generation rates (molar, volumetric, or gravimetric) are seldom reported in LT electrolysis literature (they are instead converted to $J_{product}$ and FE), which to some extent hinders the comparison of results between technologies.

The electrocatalyst material has a strong influence on product selectivity. While a wide variety of materials have been explored for selective production of CO, silver (Ag) catalysts are the most widely studied and closest to practical implementation in terms of stability and selectivity [19]. FE_{CO} values of ≥95% have been reported by several groups using Ag catalysts and optimized conditions [14,66]. The search to discover more Earth-abundant catalyst materials represents an active research field.

Various cell designs are employed in LT electrolysis research, ranging from three-electrode cells with CO_2-saturated liquid electrolytes (used for benchmarking catalyst performance), to performance-oriented devices resembling water electrolyzers or fuel cells. It has been estimated that to reach commercial viability, LT electrolysis cells should operate at current densities exceeding 200 mA/cm^2 [15]. Due to the limited solubility of CO_2 in water, typical laboratory electrochemical cells in which CO_2 is bubbled into the electrolyte cannot achieve these target currents. To achieve sufficiently high flux of CO_2, a common approach is to use a gas diffusion electrode (GDE) [15,65]. In this configuration, the porous GDE is positioned between the electrolyte (liquid or membrane) and a gas chamber, through which CO_2 can be fed directly to the catalytic surface at rates sufficient to support current densities approaching or exceeding 1 A/cm^2.

Much of the research on LT electrolysis to date has focused on understanding and improving the behavior of the cathode, rather than the full cell. In such studies, the potential-dependent activity of the cathode (working electrode) is usually reported with respect to a reference potential (reference electrode) in a three-electrode cell configuration, allowing characterization of cathode behavior without the convoluting influences of the rest of the cell. Cathode performances are typically reported in terms of the rate and selectivity of the reaction toward the product(s) of interest. In order to maintain well-controlled environments, an excess of CO_2 is often fed to the cell, meaning only a small fraction of CO_2 gets converted into product.

With efforts to develop practical electrolyzer cells for LT electrolysis, increasing attention is being paid to energy efficiency, conversion, and product yield. The applied cell voltage *E* is the primary indicator of energy efficiency, since larger voltages correspond to greater power consumption per unit product produced. Note that the two-electrode cell voltage *E* (measured between anode and cathode) differs from the cathode potential described above (which alone cannot be used to determine cell efficiencies). The energy efficiency (*EE*) of a cell can be expressed by relating the applied voltage and the FE to reversible cell voltage for the reaction of interest (E^0).

$$EE = \frac{E^0 \cdot FE}{E} = \frac{E^0 \cdot J_{product}}{E \cdot J_{tot}} \quad (12)$$

In LT electrolysis device studies, energy efficiencies are not commonly reported, nor is the energy consumption per unit product (e.g. kWh/Nm$^3_{CO}$). Both of these metrics can be simply determined from *E* and *FE* (see Supplementary Note), and would facilitate direct comparison of results between technologies (further discussed later in Section 3.1) [5]. We therefore suggest that LT device studies include these values in their reports.

The CO_2 conversion χ_{CO_2} (the molar fraction of CO_2 input which gets converted to product upon passing though the reactor) can be expressed as:

$$\chi_{CO_2} = \frac{CO_2 \text{ converted to products}}{CO_2 \text{ fed to reactor}} \quad (13)$$

In LT electrolysis, one should not simply use Eq. (1) (based on measuring $CO_{2,out}$) because there are other possible loss mechanisms leading to depletion of unreacted CO_2 (discussed below).

2.2.1. Interfaces

An LT electrolysis cell is interfaced with a power supply as well as inlets and outlets for reactant and product streams. The composition of the electrolyte, and the properties of the gas feed (e.g. flow rate,

pressure, purity) are important parameters affecting performance.

The feed rate of CO_2 gas can significantly affect the selectivity and rate of the conversion reaction. In most studies aimed at optimizing these two parameters, CO_2 is fed to the cell at rates significantly exceeding its rate of conversion, enabling high *FE* and J_{CO}. But under these conditions, the conversion χ_{CO_2} is low since the products are highly diluted in CO_2, a condition necessitating separation and/or recirculation. Higher conversion can be obtained by decreasing the rate of CO_2 supply, but this can lead to reactant depletion and subsequent decrease of J_{CO} and increase in J_{H_2}. A full systems analysis must consider this trade-off between χ_{CO_2}, selectivity, production rate and product concentration [67,68], as well as the need for downstream separation steps [17,69,70]. The CO_2 pressure is also an important parameter influencing this interplay, and while most reports operate at near-ambient pressures, a few reports have shown how elevated pressures (in the range 5–50 bar) can improve performance [71-73].

One notable challenge in LT electrolysis is depletion of CO_2 due to chemical reactions. A cathode operating at high rates in contact with aqueous electrolytes generates high local pH, which leads to the reaction of CO_2 with OH^- to form HCO_3^- and CO_3^{2-} (Eq. (14)). These anions are unreactive at the cathode, and can be transported from cathode to anode by electromigration, facilitated when using commonly-employed anion exchange membranes. At the anode, the local drop in pH shifts the equilibrium back towards CO_2 and hence a significant portion of the CO_2 feed passes through the cell unreacted [74,75]. Approaches to circumvent this loss mechanism include the use of carbonate-free or acidic electrolytes, or bipolar membranes preventing carbonate crossover, each coming with tradeoffs in performance or efficiency [76,77]. Alternatively, CO_2 could be recovered from the anode stream and recycled to the cathode [69].

$$2OH^-_{(aq)} + CO_{2(g)} \leftrightarrow CO_3^{\ 2-}(aq) + H_2O_{(l)} \quad (14)$$

Most laboratory experiments are conducted on research-grade CO_2 (N4.0–5.0, i.e. $\geq$ 99.99 – 99.999%). Impurities in the gas stream can lead to effects such as side reactions (like electrochemical reduction of the impurity species) or catalyst poisoning. A few studies have examined the influence of flue gas compositions on Ag-based LT electrolysis to CO, including SO_2, NO_x, and O_2 [78–81]. In general, they found that electrochemical reduction of the impurity species leads to decrease in FE toward CO, but the effects were reversible when using Ag catalysts. Studying the influence of simulated flue gas conditions on long term stability and performance, Van Daele et al. observed stable operation in 20 h tests, suggesting feasibility of working with impure flue gas compositions for CO_2 to CO conversion on Ag electrodes [78]. But as summarized in Harmon et al., CO-FE can decrease significantly in the presence of NOx levels >1%, wherein the side reactions lead to decreased energy efficiency since electrons go toward undesired processes [81]. Further studies over longer durations are needed, as well as technoeconomic analysis to compare the impacts of using purified or impure streams.

Liquid electrolytes are typically fed through the cell at either the anode (anolyte), cathode (catholyte) or both. Aqueous alkali metal bicarbonate solutions are commonly used (e.g. $KHCO_3$), but alkaline or acidic electrolytes are studied as well, each providing advantages and disadvantages. Acidic pH helps avoid the conversion of CO_2 to (bi)carbonate, but acidic environments tend to enhance the rate of undesired H_2 evolution. Alkaline pH can help favor CO_2 reduction over H_2 evolution, as well as minimizing cell voltages due to improved kinetics of the anode reaction, but this comes with the consequence of CO_2 consumption as (bi)carbonate, as described earlier. There are many other complex and important aspects of how electrolyte composition affects cell performance [82,83], and new scientific insights are continuously emerging. Based on the reactions for CO_2 electrolysis to CO and O_2 (Eqs. (7)–(9)), it is technically possible to operate an LT electrolysis cell with only humidified gas feeds without liquid electrolyte, or with pure water feeds, both of which could offer advantages in terms of stability and simplicity. However, electrolytes have been found to play important roles in influencing electrocatalyst and device behavior, [84] and purely gas-fed cells have not yet been demonstrated effectively.

To avoid short-circuiting of the electrodes and to mitigate product crossover (where reduced products could potentially be re-oxidized), LT electrolysis cells typically employ a separator, usually an ion exchange membrane or a porous diaphragm [76,85,86]. In contrast to the plasma route, electrochemical approaches maintain separate streams of CO and O_2, since the two half-reactions are spatially separated by this barrier and can exit the cell without mixing.

Since LT electrolysis reactors are typically operated at near-ambient pressure and temperature, they can reach steady-state operation conditions relatively quickly. An advantage of the LT approach is that the reactors can operate under fluctuating or intermittent input power, such as from a solar photovoltaic plant [87].

Since the cathode product stream is typically diluted by unreacted CO_2, and CO_2 can also be liberated in the anode outflow following carbonate crossover, effective LT electrolysis processes will likely need to incorporate product separation steps wherein this unreacted CO_2 can be captured and recycled through the cell, using technologies such as pressure swing adsorption [88,89].

2.2.2. *Lab-scale experiments vs industrial-scale setups*

As described above, lab-scale experiments are often conducted in model three-electrode cells with CO_2-saturated electrolytes, a configuration that cannot be scaled to application. Recent years have seen a significant increase in efforts toward developing devices based on GDEs which can achieve more relevant current densities. Most such studies are conducted on cells with active electrode areas on the order of 1 cm^2, with a few studies examining larger electrode areas (10–100 cm^2) as well as upscaling via multi-cell stacks [18,90–93]. At the laboratory scale, a variety of reactor configurations are still under consideration, employing different combinations of catalysts, electrolytes, membranes, and cell geometries [76,94,95].

Several entities are actively developing pilot-scale LT electrolysis systems for CO production, including research groups, start-ups, and larger companies [14]. For example, Dioxide Materials has published reports claiming excellent selectivity over extended operation (4,000 h) on 5 cm^2 devices, as well as good performance on 250 cm^2 cells [96,97]. Siemens Energy AG has reported progress in advancing LT CO_2 to CO conversion to TRL 5, developing large area cells (>3000 cm^2 active area) operating at 3–5 kW in an automated CO electrolyzer pilot plant, with goals of achieving 1 MW in the near future, and ongoing efforts with Evonik [98] to develop a modular plant to produce CO which is subsequently upgraded to specialty chemicals using bioreactors [99–101]. Overall, while the technology is approaching industrial performance, to the best of our knowledge there is not yet a commercial system available for purchase. For the pilot-scale benchmarking comparisons in Section 4, we take the results of Krause et al. [101] due to the comprehensive performance metrics provided therein, but we note that the technology is continuously advancing and further unpublished progress in performance and upscaling exists.

2.3. *High temperature electrolysis*

High temperature (HT) electrolysis refers to a device employing two electrochemically active layers separated by a solid electrolyte layer as shown in Fig. 3. The solid electrolyte is usually a ceramic oxide material with pure, that is with an ionic transfer number of 1, either oxygen ion or protonic conductivity properties. In this comparison, only oxide ion conductors are considered. The solid electrolyte layer should be gas tight to prevent the mixing of the two gas streams supplied to both electrodes on the two sides of the electrolyte. The fuel, carbon dioxide in case of CO_2 electrolysis, is supplied to the cathode, where it is reduced to carbon monoxide and an oxygen ion (Eq. (15)). The oxygen ions migrate

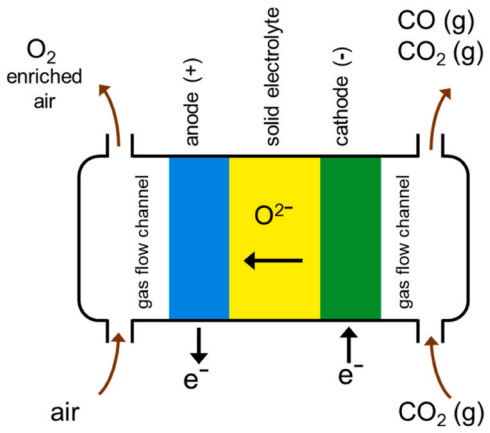

Fig. 3. Schematic representation of the HT electrolysis cell.

through the electrolyte layer to the anode, where they are oxidized to molecular oxygen (Eq. (16)). The net cell reaction is given in Eq. (17). In contrast to LT electrolysis no side reactions can occur when supplying pure carbon dioxide to the cathode, meaning that the faradaic efficiency (FE) of the CO_2 reduction reaction is 1. For each mol of CO_2 that is reduced, exactly one mol of CO is formed. High temperature (HT) electrolysis of carbon dioxide requires voltages of only 1.1 to 1.4 Volt (see Section 2.3.2).

$$CO_2(g) + 2\ \ e^- \rightarrow CO(g) + O^{2-} \tag{15}$$

$$O^{2-} \rightarrow\ \ \frac{1}{2}O_2(g) + 2\,e^- \tag{16}$$

$$CO_2(g) \rightarrow CO(g) + \frac{1}{2}O_2(g) \tag{17}$$

Due to the renewed interest in HT electrolysis, initially the materials for cells and stacks well-known from solid oxide fuel cell (SOFC) development were used. The oxygen ion conducting electrolyte is yttria stabilized zirconium dioxide (YSZ), usually with 8 mol% yttria (8YSZ). The cathode material is a mixture of metallic Ni and the ceramic electrolyte material 8YSZ, commonly referred to as a cermet (ceramic metal). The Ni is the electrochemically active material for the reduction reaction and provides the electronic conductivity in the cathode layer. The 8YSZ in the cermet prevents the Ni from agglomerating and stabilizes the porous structure of the cathode layer, which is required for the gas phase transport of the reactants (here CO_2) and products (here CO) to and from the active sites. The anode or air electrode is usually a perovskite oxide with composition (La,Sr)(Co,Fe)$O_{3-\delta}$ (LSCF) [102]. The mixed valencies of the transition metal ions on the B-sites in the perovskite structure provide electronic conductivity in the material. The Sr-substitution on the A-sites may lead to an oxygen sub-stoichiometry (δ) providing additional oxygen ion conductivity in the material as well. These materials are therefore usually referred to as mixed ionic electronic conductors (MIEC). To prevent the reaction of the LSCF with 8YSZ at high operating temperatures a gadolinium-doped ceria (GDC) barrier layer must be put in between both layers. The anode layer also must be porous to allow for the gas phase transport of the evolved oxygen away from the active sites.

2.3.1. Interfaces

The interfaces of the HT electrolysis process comprise the properties of the CO_2 feed gas (e.g. purity, pressure) at the inlet, the CO product gas at the outlet and the power required to operate the system. In order to compare with the other processes, the type of operation and the upscaling and automation aspects are also considered.

For laboratory tests on cells, stacks and demo-systems research-grade CO_2 (N4.0 or N5.0) is used. For the commercially available eCOs™-system it is stated that it is designed to operate on food or beverage grade carbon dioxide [103], which corresponds to a purity of N3.0 (i.e. ≥99.9% CO_2) [104]. Mainly from the research and development of Solid Oxide Fuel Cells it is known that Sulphur impurities in feed gasses lead to a de-activation of the Ni-YSZ cermet used as electrocatalyst on the cathode side. Sulphur concentrations in the feed gas should be below 1 ppm, which may require an appropriate cleaning step depending on the carbon dioxide source used. One other critical point is the possible re-oxidation of the Ni catalysts. In order to prevent this a reducing agent such as CO or H_2 is added to the carbon dioxide feed gas [12]. Using CO as reductant can be accomplished on the system-level by introducing a cathode gas recirculation loop, in which part of the produced CO is fed back to the CO_2 feed gas stream. This merely dilutes the CO_2 feed gas stream passing through the electrolysis cells, but has only a minor effect on the efficiency of the system. Using H_2 as reductant leads to an additional reaction, the so-called reverse water gas shift (RWGS) reaction given in Eq. (18). It is known from co-electrolysis investigations, that the CO_2 electro-reduction is partly shifted to steam electro-reduction, since this is thermodynamically favorable [12]. The product gas will in this case contain certain amounts of H_2 and H_2O next to CO and CO_2 determined by the RWGS equilibrium. It depends on the further use of the CO product gas if these can be tolerated.

$$H_2(g) + CO_2(g) \rightarrow CO(g) + H_2O(g) \tag{18}$$

The product gas usually contains CO with small amount of unreacted CO_2. This primarily depend on the CO_2 utilization, i.e. conversion, which can be as high as 95% in HT electrolysis. The Topsøe eCOs™-system standard layout offers 99.0 vol% pure CO, with major impurities being CO_2, CH_4, O and H_2O typically below 5 ppm. With special modifications, the eCOs™ units can deliver purities as high as 99.999 vol% (N5.0) [103].

2.3.2. Lab-scale experiments vs industrial-scale setups

Lab-scale experiments on Solid Oxide Electrolysis Cells (SOEC) are mainly conducted on single cells and on (short-)stacks. These experiments all require a furnace in order to maintain the operating temperature. Single cells investigated are usually button-type cells with a diameter of 20 mm or square cells with dimensions up to 50×50 mm^2. These cells are placed in all ceramic sample holders as described previously [105,106]. Short-stacks are usually built up with 4 or 5 layers, with one cell with the dimensions 100×100 mm^2 in each layer as described in [107].

Fig. 4a shows current-voltage characteristics of commercially available single cells (Elcogen®, Tallinn, Estonia) for pure CO_2-electrolysis in comparison with steam- and co-electrolysis [105]. The cells consisted of a nickel oxide/8 mol% yttria-stabilized zirconia (NiO/8YSZ) cermet cathode that was reduced at 900 °C in hydrogen to Ni/8YSZ, an YSZ electrolyte and a lanthanum strontium cobaltite (LSC) anode. In order to prevent reactions of the anode and electrolyte materials, a gadolinium-doped ceria (GDC) barrier layer was included between anode and electrolyte [106].

Fig. 4b shows the same comparison for cells in a five-layer short-stack [107]. Commercially available half-cells from CeramTec (Marktredwitz, Germany) were used in this stack. The diffusion barrier and air electrode layer were added in-house. These cells consisted of a porous support backbone (~300 μm) made of a Ni(O)/8YSZ cermet by means of tape casting, followed by a functional layer of fuel electrode material from the same material, but with a finer microstructure, a dense ceramic electrolyte layer of about 10 μm thickness made of 8YSZ, a diffusion barrier layer from a screen-printed GDC and, finally, a screen printed LSCF air electrode [107].

The IV-characteristics in Fig. 4 show both a lower performance for CO_2-electrolysis in comparison to steam- and co-electrolysis. This can be deduced from the steeper slope (i.e. cell resistance) for the CO_2-electrolysis IV-characteristics as well as from the lower current-densities that can be reached at a fixed cell voltage. These observations are

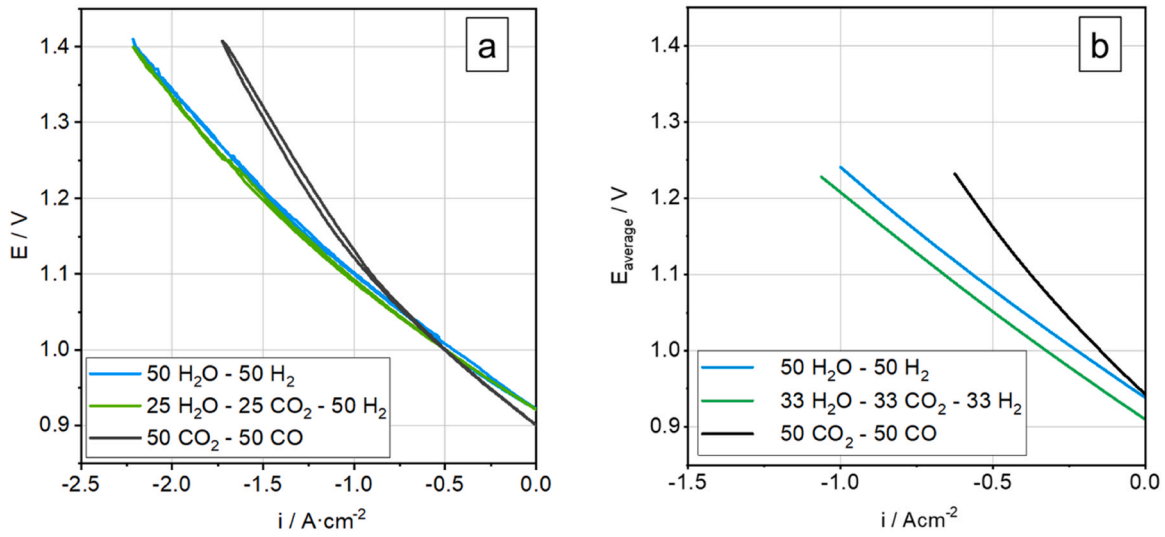

Fig. 4. Current-density / voltage characteristics for Solid Oxide Electrolysis Cells operated in steam- (blue), CO_2- (black) and co-electrolysis (green). a) single cell (Ni-YSZ/YSZ/CGO/LSC) measured at 900 °C (adapted from [105]), b) average voltage per cell in a short-stack with five cells (Ni-YSZ/YSZ/CGO/LSCF, 10×10 cm^2; 80 cm^2 effective area) measured at 800 °C (adapted from [107]).

consistent with many previously reported studies on CO_2- and co-electrolysis like [5,12,13,34,108,109]. In a recent detailed study on the boundary region from co-electrolysis towards pure CO_2-electrolysis it was shown that above 30% steam in the feed gas the performance equals that of pure steam-electrolysis. This is all because of the RWGS reaction (see Eq. (18)) which is much faster than the electrochemical reduction reactions [110]. For very low steam content (< 4,7%) the performance is similar to pure CO_2-electrolysis, which is considerably lower because of the slower kinetics for the CO_2-reduction reaction [110].

The differences in performance between the single cell (Fig. 4a)) and the short-stack (Fig. 4b)) are mainly due to the additional components (interconnect and contact layers) leading to additional (contact) losses in the stack. One other difference is the air electrode material used, i.e. LSC in the single cells and LSCF in the cells used in the short-stack. In general, the LSC air electrode enhances the performance of the SOEC compared to LSCF.

Reports on lab-scale experiments on full SOEC systems and demonstration units in a multi kW-class power range are limited. An overview can be found in [111], which also reports on the results of a 10/40 kW-class reversible Solid Oxide Cell demonstration system. The demonstration system could be operated in reversible mode, i.e. both fuel cell as well as electrolysis operation, with hydrogen and steam, respectively, on the fuel side of the solid oxide cells. In fuel cell mode, the system could provide an electrical output power from 1.7 to 13 kW_{AC}. The maximum system efficiency of 63.3% based on the lower heating value (LHV) of hydrogen could be reached at a system power of 10.4 kW_{AC}. In electrolysis mode, a maximum efficiency of 71.1% (LHV) was achieved with an electrical power input of −49.6 kW_{AC} [111].

For the comparison with the LT CO_2-electrolysis and the CO_2 plasma

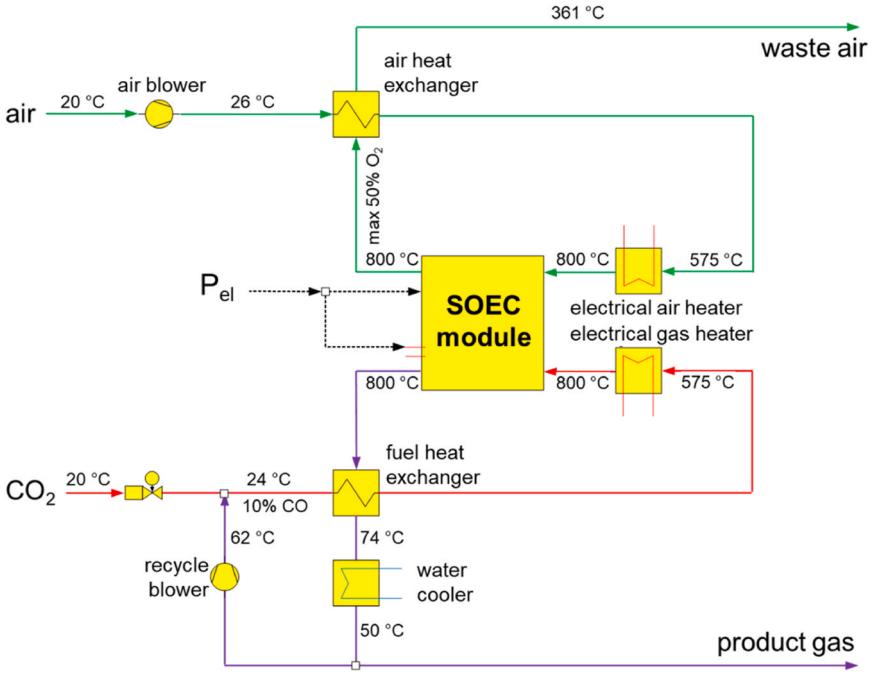

Fig. 5. Simplified flow scheme of a multi kW-class SOEC system for CO_2-electrolysis (adapted from [111]).

conversion technologies described in Section 4 the system layout from [111] was adapted to pure CO_2-electrolysis. This simplified flow scheme of a 70 kW SOC system for CO_2-electrolysis is shown in Fig. 5. The major difference being the omission of the steam generator. For the calculations of the parameters needed for the comparison in Section 4, the performance of the SOC module was taken from the IV-characteristics measured at 800 °C in the short-stack as described above and shown in Fig. 4b. A current density of 1.0 A/cm^2 was taken and the CO_2-utilisation, which equals the CO_2-conversion, was set at a maximum value of 86% to prevent any carbon formation, which might occur at higher conversion ratios. This results in an CO outflow of 17.5 m^3/h with an electrical input to the stack of 69.6 kW. The wall plug efficiency amounts to 89.0% with an electric power consumption (EPC) of 3.89 kWh/Nm$^3_{CO}$. For the calculation of the wall plug efficiency an inverter and rectifier efficiency of 0.95 was assumed.

The only industrial-scale setup currently available is the eCOs™ system from the Danish company Haldor Topsøe A/S (HTAS). For the comparison in Section 4 available data were taken from [39,103].

3. Benchmarking parameters relevance and grouping

In this section we describe the methodology and parameters used for this benchmarking exercise. For this exercise the goal is to compare the relevant technologies for CO_2 conversion with CO, CO_2 gas mixture as an outflow gas, and with quantified CO gas outflow. To achieve a targeted CO_2, CO gas mixture, in case of plasma conversion technology and LT electrolysis an additional step of gas removal is required: O_2 separation, and some H_2 and H_2O vapor, respectively. Finding suitable parameters to compare the two different technologies (electrolysis and plasma conversion technology) is a complex task, as each technology has some commonly used figures of merit (as discussed in Sections 2.1, 2.2, and 2.3). Even comparison between low- and high-temperature electrolysis is a challenge as each technology originates from a different scientific field with own longstanding conventions [5].

The main norm to identify a suitable comparison criteria is that it should be comparable across technologies, measurable, and relevant for industrial application. The identified parameters are described in the following sections and are grouped in three categories:

- Performance of each technology in terms of efficiency of the CO production
- Interface requirements in terms of industrial application
- Economic consideration

In the following sections, the identified parameters are marked in bold so they can be easily found in the text and correlated with the results summary shown in Table 1 and Table 2.

3.1. Performance comparison

For the performance comparison several parameters are identified as suitable for demonstrating the performance of each technology. **Technology readiness level (TRL)** indicates the development stage of the technology, and fair comparisons of performance metrics are best performed between technologies at similar TRL [112]. The size of the reactor and its output are not determining factors for identifying TRL. **CO_2 conversion** (χ_{CO_2}) is a measure of the CO_2 inlet gas conversion as described in Section 2.1 (Eq. (4)) for plasma conversion technology and 2.2 (Eq. (13)) for LT and HT electrolysis. The **CO outflow** can be either calculated as a product of the CO_2 conversion and the CO_2 inflow ($\Gamma_{CO} = \chi_{CO_2} \cdot \Gamma_{CO_2}$), or it can be measured directly.

The efficiency of a process is a measure of amount of energy input to drive the desired reaction compared to its standard thermodynamic energy, typically expressed in percentage. In case of CO_2 conversion, this refers to the energy used to dissociate CO_2 molecules into CO and O_2 molecules (Eq. (1)). The efficiency is a parameter that is however expressed differently for electrolysis and for plasma conversion. In the plasma conversion community, the **energy efficiency** is expressed in Eq. (5) in Section 2.1, while for LT and HT electrolyzers, the efficiency of the process is expressed in Eq. (12) in Section 2.2. When considering the total power required to sustain the process power supply and all other peripheral devices (pumps, flow meters, cooling/heating devices etc.), the **wall-plug efficiency** is defined using Eq. (6) in Section 2.1. **Faradaic efficiency** is the only parameter that does not have an equivalent for the plasma conversion technology, however it is an important parameter in electrolysis. In the context of CO_2 conversion, faradaic efficiency is defined as the fraction of total electrolysis current that is used towards reducing CO_2 to CO described by Eq. (11) in Section 2.2 [5]. Since in HT CO_2-electrolysis no side reactions can occur, the

Table 1
Performance comparison for LT electrolysis, HT electrolysis, and plasma conversion technology for comparison parameters described in Section 3.1. For LT and HT temperature electrolysis, two performances are provided: for lab-scale devices and for industrial-scale device. For plasma conversion technology three examples are provided: process without gas separation, process with gas separation and the high TRL example. [a] Overview based on examples compiled in Table S1 in Supplementary Note. [b] Note that numbers are not consistent, as under normal conditions η_{tot} is inversely proportional to EPC_{tot}, with $\eta tot = 100\% \rightarrow EPC_{tot} = 3.51$ kWh/Nm$^3_{CO}$.

	Low-temperature electrolysis		High-temperature Electrolysis		Plasma conversion		
	Lab-scale[a] (1-10 cm^2, 1-12 W)[95, 116]	Pilot-scale (300 cm^2, 240 W) [101]	FZJ (70 kW)	HTAS eCOs™ [39, 103]	MW plasma reactor (3 kW)	MW plasma reactor with membranes (3 kW)	KEROGREEN (6 kW) [63]
TRL	4	5	4	8	4	3	5
CO_2 conversion [%]	20-60	35	86.6	> 95	up to 56	up to 26	14
CO outflow [Nm^3/h]	0.001	0.023	17.5	6-200	0.22	0.12	0.56
Wall-plug efficiency [%]	N/A	N/A	89.0	90[b]	up to 18	up to 10	N/A
Energy efficiency [%]	30-60	25-35	94.6	> 90	up to 27	up to 18	34
Faradaic efficiency [%]	90-99	95	100	100	N/A	N/A	N/A
$EPC_{process}$ [kWh/Nm$^3_{CO}$]	8-12	10.2	N/A	N/A	12	19	11.4
EPC_{tot} [kWh/Nm$^3_{CO}$]	N/A	N/A	3.89	6-8[b]	19.8	35	N/A

Table 2
Comparison of the interfaces for LT electrolysis, HT electrolysis, and plasma conversion technology for comparison parameters described in Section 3.2.

		Low-temperature electrolysis	High-temperature electrolysis		Plasma conversion
			FZJ	HTAS eCOs™	
Input	Gas-in composition	CO_2 + H_2O	CO_2 + CO (5-10%)	CO_2	CO_2
	Required gas purity	99,99%	99,99%	99,9 %	≥98 %, dry CO_2
	Type of operation	Continuous or intermittent	Continuous with variable power input		Continuous or intermittent
	Warm-up times	Minutes	Cold - 4-6h, Hot stand-by ~minutes		Minutes
	Standby power consumption	No standby required	Hot standby required + some gas flow		No standby required
	Run-time, lifetime	Tested up to 4000 h	Tested up to 8000 h		Tested up to 29.3h Magnetron lifetime – 8000h
Output	Gas-out composition	CO_2, CO, H_2, H_2O	CO_2, CO	Standard unit 99.0 vol% pure CO, w/ CO_2, CH_4, O_2, H_2O < 5ppm. Special modifications, purities as high as 99.999 vol%	CO_2, CO, O_2
	Separation steps required (towards CO and CO_2)	Yes (H_2, H_2O)	no		Yes (O_2)
	Gas-out pressure	1-50 bar	1 bar		1 bar
Scaling	Upscaling	Stacking	Stacking, modular unit		Modular concept, up-scaling (larger power per unit)
	Turnkey process	Yes	Yes		Not achieved yet

faradaic efficiency is 100% for this technology.

A key metric that is independent of the process, which can be calculated by measuring the total power consumed and the CO outflow, is the **electric power consumption (EPC)** [113]. EPC [kWh/Nm^3_{CO}] is defined as an energy (in kWh) required to produce one normal cubic meter of CO (in Nm^3_{CO}), and two values can be distinguished: $\mathbf{EPC_{reactor}}$ considers only the power deposited in the chemical process happening inside of the reactor (plasma, electrolyzer) (Eq. (19)), while $\mathbf{EPC_{total}}$, (Eq. (20)), considers the total power required to power the process power supply and all other peripheral devices (pumps, flow meters, cooling/heating devices etc.).

$$EPC_{reactor} = \frac{power\ consumed\ in\ reactor}{\chi_{CO_2} * \Gamma_{CO_{2,in}}} = \frac{power\ consumed\ in\ reactor}{\Gamma_{CO_{out}}} \tag{19}$$

$$EPC_{total} = \frac{total\ power\ consumed}{\chi_{CO_2} \cdot \Gamma_{CO_{2,in}}} = \frac{total\ power\ consumed}{\Gamma_{CO_{out}}} \tag{20}$$

3.2. Interfaces

The interface comparison encompasses considerations of the environment in which the technology operates, including inputs and outputs. At the inlet side the properties of the CO_2 gas and electrical power are considered. The **gas-in composition** defines input gases required by the process. **Required gas purity** considers the tolerable level of impurity species which might affect the performance of the process, or degrade the components over longer time periods, defining potentially suitable CO_2 gas sources (direct air capture, point source capture, CO_2 underground storage etc.).

Type of operation indicates whether a technology favors continuous operation or if it can be intermittently started and stopped in response to fluctuating power supply or CO demand. For industrial application, stable long-term operation is necessary, demonstrated by performing long-term tests in a controlled environment (**run-time**) or identifying the life time of critical components (**lifetime**). For intermittent operation (e.g. when driven by renewable electricity sources), the times at which the technology can be switched on and brought to a required operational level is defined by **warm-up time**. In case of intermittent operation, **standby power consumption** should also be considered as it adds to the total power consumption. It refers to the power required for maintaining the device in a standby that allows faster switch-on times.

On the outlet side the produced CO gas should be delivered in a form suitable for further processing, which considers the purity of the CO gas and the pressure. In this work the microwave-induced CO_2 plasma splitting with oxygen separation is compared to the gas stream on the cathode of the electrolysis technology. Therefore **gas-out composition** at the outlet of the process is considered (plasma effluent or on the cathode for electrolysis technology), and **separation steps required** to deliver a gas containing CO and CO_2. **Gas-out pressure** is also considered as a relevant parameter when considering further process in a chain that might require a feed gas mixture at pressures above atmospheric pressure.

Since the CO_2 conversion technology is to be incorporated in a larger installation, the aspects such as **upscaling** of the technology and automation (**turnkey process**) are also considered.

3.3. Economic comparison

A common techno-economic assessment typically utilizes a process modeling tool for **process optimization and conceptual design**, in order to estimate the capital cost, the operating cost, and the revenue based on technical and financial parameters. There is however considerable uncertainty related to economic aspects of the technologies that are below TRL 6 (Technology demonstrated in relevant environment) or TRL 7 (System prototype demonstration in operational environment). As discussed later in Section 4, the lab-scale experiments compared here are at TRL of 4, thus only a preliminary consideration of capital expenditure (**CAPEX**) and operational expenditure (**OPEX**) have been performed for the three technologies. One of the aspects for an initial investment in a technology are the requirements for critical raw materials. These materials are either required in the power supplies, or in the specialty materials such as custom designed membranes and catalysts. At the operational level, the cost of production of the desired CO derived product will depend on the prices of CO_2 gas and electricity.

4. Results of the benchmarking

The results of the comparison are provided below, grouped by types of parameters: performance, interfaces, economic. For each technology at least two examples are given, one for lab-scale experiments and the other for pilot- or industrial-scale (details in Sections 2.1.2, 2.2.2, and 2.3.2). For the LT electrolysis at lab-scale we provide values compiled from a collection of recent publications, and for the HT electrolysis a lab-scale experiment at Forschungszentrum Jülich (FZJ) is presented. For the plasma conversion technology, two examples of lab-scale experiments are operated at the Max Planck Institute for plasma physics (IPP). One is the microwave plasma torch as an example of MW plasma reactor with the highest conversion currently achievable at atmospheric pressure obtained using the cooled effluent channels as shown in Fig. 1a) (MW plasma reactor). The other experiment with a nozzle is an example of MW plasma reactor with relatively high conversion with an additional oxygen separation step shown in Fig. 1c) (MW plasma reactor with membranes).

In the following tables, to emphasize the comparison of results, dark shading is used to indicate metrics where a certain technology performs notably better other technologies, while light shading indicates where metrics are comparable between technologies.

4.1. Performance comparison

Table 1 shows the performance comparison for the three technologies according to parameters described in Section 3.1. Here it is important to note that the scales of the reactor power used in the lab-scale experiments vary considerably, about 10 W for LT electrolysis, up to 3 kW for the plasma conversion, and 70 kW for the HT electrolysis. The first row contains information about the TRL of each considered process. It is followed by the results for maximum obtained CO_2 conversion and CO outflow. For LT electrolysis and plasma conversion the maximum values of efficiency and conversion are not obtained simultaneously [11,101], therefore the entries in Table 1 are either represented as a range or as a highest value achieved. Wall-plug efficiency, energy efficiency and faradaic efficiency are shown in the next rows, representing different measures of the process efficiency. Finally, the last row contains information about the electric power consumption, both for $EPC_{reactor}$ and EPC_{total}, since for some technologies either one or the other is measured. All entries that could not be determined are marked as not available (N/A).

The TRL of the lab-scale experiments (LT literature, FZJ, IPP) is estimated to be 3–4: MW plasma reactor with membrane is an experimental proof-of-concept (TRL 3), while other lab-scale experiments have been validated in laboratory environment (TRL 4). Similarity of the TRL indicates that the comparison among different technologies has merit. The TRL of the following examples from pilot or industrial applications spans a broader range, TRL 5–8. The plasma conversion setup of KEROGREEN is estimated to be TRL 5 [64], being the first plasma setup validated in relevant environment. The Siemens Energy LT setup is estimated to have TRL 5 [99,101], and the HTAS eCOs™ has TRL of 8, being an actual system completed, qualified, and commercially available. The span of TRLs should be considered when comparing the experimental and industrial technologies in terms of power levels and output.

The values of CO_2 conversion differ strongly for each technology. For HT electrolysis conversion above 85% is achieved, reaching above 95% for the industrial setup. The maximum conversion up to 56% can be achieved in a plasma torch, a setup in which the oxygen removal has not yet been tested. In the plasma torch setup with oxygen removal conversions up to 26% are achieved. In the LT electrolysis, conversions up to 60% are achieved. While higher conversions are generally favored in catalytic processes, in LT CO_2 electrolysis this usually come at the expense of decreased CO FE due to H_2 evolution [67]. For all technologies, recirculation of non-converted CO_2 (i.e. exhaust gas recirculation) is a possibility with aim to avoid CO_2 waste and maximize output [69,70].

The CO outflow strongly depends on the scale (size and power) of the setup. HT conversion ranges from 17 Nm^3/h for the FZJ HT setup, and up to 200 Nm^3/h for industrial setups [114]. For plasma conversion, the CO outflow are in range of 0.12 to 0.56 Nm^3/h. In the LT electrolysis, CO outflow is about 0.001 m^3/h for most lab-scale reports (more details in Supplementary Note), up to 0.023 m^3/h for some pilot-scale demonstrations [91,101]. Recently, Siemens Energy has claimed similar performance from a further scaled-up stack, reaching CO outflow of approx. 0.57 Nm^3/h [91,101]. It is clear that the CO outflow is strongly correlated to the size (i.e. power) of the experiments, being smallest for the 10 W LT electrolyzer and largest for the 70 kW HT electrolyzer. The output can be increased by upscaling as discussed in Section 4.2.

The wall-plug efficiency (where available) and energy efficiency are proportional to the conversion, according to the equations in Section 2.1, therefore the highest efficiencies are obtained for HT electrolysis, above 89% (lab-scale) and 90% (industrial-scale) [5], which is rather predominantly due to the fundamentals of the reaction when run at high temperature, based on internal utilization of heat [5]. These are followed by efficiencies of the LT electrolysis (30–60%). The efficiencies of the plasma conversion are in range from 18–34%. Faradaic efficiencies are above 90% for LT electrolysis and 100% for HT electrolysis. The values of wall-plug efficiency indicate that HT electrolyzer reactors are well optimised. The LT electrolyzer and plasma reactors improvement is still possible since these are technologies in development, indirectly demonstrated by a relatively low TRL level of the available pilot- or industrial-scale examples. These technologies might never reach the performance level of the HT electrolyzers, but future developments aim at reducing the current gap in the wall-plug efficiency.

The best results for the EPC_{total} are obtained with the HT electrolysis, which is a consequence of the high conversion and efficiency of the process. With the lab-scale experiment a value of 3.89 kWh/Nm^3_{CO} is measured, which is lower than the industrial-scale setup at 6–8 kWh/Nm^3_{CO} [115]. Even though the conversion and efficiencies of the LT electrolysis and plasma conversion are lower than the values obtained for the HT electrolysis, the EPC does not differ drastically. The results for the EPC_{total} of the MW plasma reactor are 19.8 kWh/Nm^3_{CO}, and the setup of the MW plasma reactor with membranes are 35 kWh/Nm^3_{CO}. No data for EPC_{total} for an industrial plasma conversion setup is available. For LT electrolysis only $EPC_{reactor}$ has been determined (see below); for the pilot-scale setup it is at approximately 10 kWh/Nm^3_{CO}, and lab-scale reports typically span 8–12 kWh/Nm^3_{CO}.

Regarding LT electrolysis, estimating the wall plug efficiency and EPC_{tot} requires consideration of energy consumption by peripheral components besides the cell stack, such as pressure/flow control, thermal management, and product separation, which is difficult to do at this

stage of development. While several technoeconomic analysis articles for LT CO_2 electrolysis have been reported, to our knowledge none have examined the specific energy requirements for the peripheral components, which make it difficult to properly estimate EPC_{tot} [88,89,116]. Those analyses focused on economic aspects, using the assumption that LT CO_2 electrolyzer CAPEX and OPEX will likely be comparable to that of alkaline electrolyzers. One additional key component important in CO_2 electrolysis implementations is the separation of unreacted CO_2 from the product(s) in the cell outflow. Analyses claim separating CO_2/CO gas mixtures by pressure swing adsorption would demand approx. 0.25 kWh/Nm^3 [88], which is comparatively small compared to the energy used by the cell itself ($EPC_{process}$) and suggests that the electrolyzer cell will dominate the energy consumption in LT CO_2 electrolyzers [69].

By directly reporting the energy input needed per unit of product, the EPC facilitates comparison and estimation of operating costs of different technologies, and it is hence a recommended parameter to report in future publications. Low values of the EPC_{tot} for the HT electrolysis reflect high level of optimization and upscaling achieved, in addition to favorable thermodynamic conditions [5]. EPC values for the LT electrolyzer and the plasma reactors demonstrate that the technologies are not lagging far behind from the HT electrolyzers, however further optimization in performance and upscaling are necessary.

4.2. Interfaces

Table 2 shows the performance comparison for the three technologies according to the parameters described in Section 3.2. The requirements for the LT electrolysis and plasma conversion for lab-scale and industrial-scale setups are similar thus the information is presented in a single column. For the HT electrolysis the difference for certain parameters for the lab-setup and industrial setup is still present, thus the data are presented in two columns.

Interface-related parameters have been split up into three groups (input, output, and scaling) in Table 2. The first group consists of process input parameters, considering the properties of CO_2 gas delivered to the process and the type of operation. The second group are the parameters relevant for the output, including gas composition, pressure, and separation steps. Upscaling of the technology and automation (turnkey process) are also considered.

The gas-in composition differs for each technology. LT electrolysis requires CO_2 gas mixed with some water, the purity of CO_2 gas of 99.99% is typically employed, since the presence of O_2 or flue gas impurities can lead to a decreased CO FE (due to side reactions), worsening the cell efficiency (more details are provided in Section 2.2.1). The HT electrolysis lab-scale setup at FZJ requires CO_2 mixed with 5–10% of CO. The necessary CO gas is required only at the beginning of the process, while after ignition it is delivered from the CO outflow. Here CO_2 with a purity of 99.99% is used in the laboratory, and the sulphur content should be lower than 10 ppm. The gas purity required for the industrial-scale HT electrolysis is food or beverage grade CO_2 at 99.9% [115]. For the plasma conversion a 98% dry CO_2 purity is required, as discussed in Section 2.1.1.

Two types of operation are considered, continuous and intermittent, depending on the source delivering the power to the process as well as the demand for CO production. The warm-up times of the LT electrolysis and the plasma conversion are typically measured in minutes. Thus, for these two technologies minimal standby power is required. The starting times of the HT electrolysis differentiate between the cold start-up, which requires 4–6 hours, and the hot start-up that requires minutes until reaching a required operational level. The hot standby of the HT electrolysis requires to maintain the temperature of the electrolyzer cell at or close to the operational temperature of 700–800 °C, and a minor reducing gas flow is required to stream through the electrolyzer cell. Run-time of the LT electrolysis has been tested up to 4000 hours [14], and up to 8000 h for the HT electrolysis. The long-term operation of the plasma conversion has only been tested recently with the plasma operated intermittently for a duration of 29 hours and 20 minutes in total, nevertheless the performance was consistent for the whole duration of the test [43]. For the plasma conversion, if the microwaves are generated using the magnetron, the lifetime of the magnetron is rated at 8000 hours. If the solid-state power supplies are used for the microwave generation, the lifetime of the solid-state power supply is several years [117].

Gas out composition differs for each technology. In LT electrolysis, the output on the cathode includes CO, unreacted CO_2, H_2O vapor, and some H_2 produced by water reduction. Trade-offs between conversion and side reactions make pure product streams challenging to achieve, so separation steps are likely needed. Pressures demonstrated at the output side of the LT electrolysis range from 1 to 50 bar, although at the higher pressures there is a lack of long-term operational data. In HT electrolysis, the absence of liquid electrolyte results in a pure CO stream on the cathode with a few percentages of unreacted CO_2 for which no additional separation stages are required. The output pressure is 1 bar. For the plasma conversion, the output gas is a mixture of CO_2, CO and O_2, thus the separation step to remove O_2 is required. The pressure at the output is atmospheric pressure.

Upscaling of both electrolyzer technologies is typically done by increasing electrode area and stacking multiple cells to increase the operating power and CO output [18,107]. System automation in the sense of a simple turnkey process that can be easily installed and run automatically has been demonstrated for HT electrolysis, and efforts are underway for the LT approach. For the plasma conversion technology up-scaling can be done be either be stacking multiple plasma modules (consisting of independent power supply and plasma torch) in parallel, or by upscaling the power and flow through a single plasma module, either using larger power supplies (max. 15 kW for the 2.45 GHz frequency) or lowering the frequency to 915 MHz (100 kW power supply available). For the plasma torch the turnkey status is not yet achieved. The reliable ignition of the plasma and the operation of the oxygen separation membranes is still under development.

Assessment of the space required for installation of each technology is considered, but it is strongly dependent on the designated power and CO outflow, thus any estimates are very speculative. No major reasons were identified for the technologies considered that would provide an obstacle for the integration in a larger production installation.

4.3. Economic comparison

The lab-scale experiments compared here are at TRL 4, thus only a preliminary consideration of capital expenditure (CAPEX) and operational expenditure (OPEX) could be done. In terms of CAPEX, the critical raw materials are identified as a possible factor that has the strongest impact. For LT electrolysis, elements Ag and Ir are used for electrocatalysts, as well as perfluoroalkoxy alkane (PFA) components for membranes. For HT electrolysis, the elements Gd, Ce, Ni and Co are required for the solid oxide cells. In plasma conversion, the oxygen separation membranes contain materials La, Ca, Co, Ce, Gd, which should be all relatively easy to recycle [118]. For all technologies the power supplies will contain some critical raw materials in small quantities (Pb (<0.3%), Cd (<0.02%), Ag (<0.001%), and in traces: Au, Pd, In, Hg, Br) [119].

The main OPEX are influenced by the CO_2 gas cost (mainly depends on the source of CO_2 and taxation schemes), electricity cost, and the cost and lifetime of consumable components and materials. Regarding electricity, since wholesale electricity prices show strong intraday variations (e.g. low electricity price in period with strong wind or sun), there are likely advantages to technologies which can run intermittently (plasma and LT), taking advantage of discounted costs during periods while shutting down during expensive periods. Conversely, processes running continuously would face higher average electricity prices. Ultimately the optimal operation mode will depend on numerous other factors,

including CO_2 supply, CO demand, and the downstream process, and hence different technologies will likely fit best into different application niches.

In the LT electrolysis, membranes and catalysts require periodic replacement. In the HT electrolysis the sub-stack components might require replacement. In the plasma conversion the oxygen separation membranes require replacement, and the magnetron of the microwave power supply requires replacement every 8000 h [117]. It is worth mentioning that the magnetron is only a single component of the plasma setup that is technically relatively easy to replace, while the rest of the setup is not affected by such maintenance.

5. Summary and conclusion

A benchmarking of the atmospheric pressure microwave-induced CO_2 plasma splitting with electrochemical CO_2 conversion, both LT and HT electrolysis, is presented. For each technology at least two examples are discussed. One example is for the lab-scale experiment and the other is the industrial-scale setup currently available, being at a different TRL for the three technologies. For the plasma conversion technology, two examples of a lab-scale experiment are given, one is an example of a MW plasma reactor with the highest conversion currently achievable at atmospheric pressure (MW plasma reactor). The other experiment is an example of a MW plasma reactor with relatively high conversion and an additional oxygen separation step (MW plasma reactor with membranes). The oxygen removal step is necessary in order to compare the output of the plasma conversion (CO and CO_2 gas mixture) with the output of the electrochemical reactor (typical gas mixture on cathode containing CO_2 and CO). A set of parameters suitable for comparison of three different technologies is identified, and grouped in three categories: performance, interfaces and economic aspects.

In the performance comparison it is established that the lab-scale experiments are all on TRL level 4 which makes their direct comparison possible. Comparing the total electric power consumption (EPC_{total}) the values obtained for plasma conversion for the lab-scale experiment of about 20 kWh/Nm^3_{CO}, whereas the values for the HT electrolysis are lowest, at around 4 kWh/Nm^3_{CO}. For LT electrolysis only $EPC_{reactor}$ has been determined for the lab-scale reports, and typically it spans 8–12 kWh/Nm^3_{CO}. These $EPC_{reactor}$ values are very similar to the values obtained for the plasma conversion lab-scale experiment at 12–19 kWh/Nm^3_{CO}. Given the potential of LT electrolysis and plasmas to use intermittent electricity, it is necessary to develop a deeper understanding of these processes and optimize these technologies.

The key features of the plasma conversion technology are relatively high conversion (up to 56%) and moderate energy efficiencies (up to 27%). The CO_2 gas of reduced purity of only 98% can be used without decrease of the performance, which is consistent with the CO_2 purity coming from DAC sources. However, the performance is very sensitive to water vapor, thus dry CO_2 must be used. Fast switching time on the order of minutes, and no need for hot standby indicate that plasma conversion is particularly suitable for an intermittent type of operation. Consistent performance over extended periods, and the longer run-time test indicate suitability for continuous operation. The aspects that require further development are optimization of the process towards lower EPC_{total} values, improved oxygen gas separation, and reliable ignition of the plasma.

The key features of the LT electrolysis technology are moderate conversion (up to 60%) and energy efficiencies (up to 60%). Similar to the plasma conversion, fast switching time in the order of minutes, and no need for hot standby indicate particular suitability for an intermittent type of operation [87]. From the compared technologies for CO_2 conversion, only LT electrolysis has demonstrated significantly pressurized output gas, reaching up to 50 bar. Aspects requiring further development include stability, energy efficiency, carbon efficiency, and separation of side products (H_2, H_2O).

The key features of the HT electrolysis technology are high conversion (86%), and energy efficiency (up to 85%), leading to the lowest EPC_{total} of 3.89 kWh/Nm^3_{CO}. The CO outflow is also highest of all technologies, however it is strongly correlated to the size of the lab-scale experiment (i.e. power input), as these ranges from 10 W (LT electrolysis) over 3 kW (plasma conversion) to 70 kW (HT electrolysis). High temperature operation requires long start up times from cold (4–6 h) whereas in hot-standby start up is reduced to minutes. This feature of the HT electrolysis indicates that this technology is most suitable for continuous operation.

Declaration of Competing Interest

The authors declare that they have no known competing financial interests or personal relationships that could have appeared to influence the work reported in this paper.

Data availability

Data will be made available on request.

Acknowledgments

LGJdH would like to thank the co-workers Roland Peters and Robert Deja for conducting the process engineering calculations for the HT CO_2-electrolysis case. MTM and SG acknowledge the Helmholtz Association's Initiative and Networking Fund (Helmholtz Young Investigator Group VH-NH-1225 and the Helmholtz Climate Initiative HI-CAM). AH would like to thank Arne Meindl for fruitful discussions. The framework for the comparison is the milestone 2.1 defined within Helmholtz PoF IV cross-center research program in the field "Energy", research program "Materials and Technologies for the Energy Transition" (MTET), topic "Chemical Energy Carriers": "Integration of microwave-induced CO_2 plasma splitting with oxygen separation to deliver a gas suitable for fuel synthesis and benchmarking with electrochemical CO_2 reduction with a view to energy efficiency and cost". The authors are responsible for the content of this publication.

Appendix A. Supporting information

Supplementary data associated with this article can be found in the online version at doi:10.1016/j.jcou.2024.102825.

References

[1] IEA, World Energy Outlook 2021, IEA, Paris, 2021. ⟨https://www.iea.org/reports/world-energy-outlook-2021⟩.
[2] C. Wulf, P. Zapp, A. Schreiber, Review of Power-to-X Demonstration Projects in Europe, Front. Energy Res. vol. 8 (2020).
[3] C. Schmid, A. Hahn, Potential CO2 utilisation in Germany: An analysis of theoretical CO2 demand by 2030, J. CO2 Util. vol. 50 (2021) 101580.
[4] A. Schreiber, A. Peschel, B. Hentschel, P. Zapp, Life Cycle Assessment of Power-to-Syngas: Comparing High Temperature Co-Electrolysis and Steam Methane Reforming, Front. Energy Res. vol. 8 (2020).
[5] R. Küngas, Review—Electrochemical CO2 Reduction for CO Production: Comparison of Low- and High-Temperature Electrolysis Technologies, J. Electrochem. Soc. vol. 167 (2020) 044508.
[6] M. Bachmann, S. Völker, J. Kleinekorte, A. Bardow, Syngas from What? Comparative Life-Cycle Assessment for Syngas Production from Biomass, CO2, and Steel Mill Off-Gases, ACS Sustain. Chem. amp; Eng. vol. 11 (2023) 5356–5366.
[7] B. de Haart, U. Fantz, A. Hecimovic, A. Schulz, A. Navarrete Munoz, M. Klumpp, Trendbericht Technische Chemie 2021, Nachr. aus der Chem. vol. 69 (2021) 52–59.
[8] A. Fridman, Plasma Chemistry, Cambridge University Press, 2008.
[9] A.J. Wolf, T.W.H. Righart, F.J.J. Peeters, P.W.C. Groen, M.C.M. van de Sanden, W.A. Bongers, Characterization of CO2 microwave plasma based on the phenomenon of skin-depth-limited contraction, Plasma Sources Sci. Technol. vol. 28 (2019) 115022.
[10] A.J. Wolf, F.J.J. Peeters, P.W.C. Groen, W.A. Bongers, M.C.M. van de Sanden, CO2 Conversion in Nonuniform Discharges: Disentangling Dissociation and Recombination Mechanisms, J. Phys. Chem. C. vol. 124 (2020) 16806–16819.

[11] F.A. D'Isa, E.A.D. Carbone, A. Hecimovic, U. Fantz, Performance analysis of a 2.45 GHz microwave plasma torch for CO2 decomposition in gas swirl configuration, Plasma Sources Sci. Technol. vol. 29 (2020) 105009.

[12] Y. Song, X. Zhang, K. Xie, G. Wang, X. Bao, High-Temperature CO2 Electrolysis in Solid Oxide Electrolysis Cells: Developments, Challenges, and Prospects, Adv. Mater. vol. 31 (2019).

[13] W. Li, J.-L. Luo, High-Temperature Electrochemical Devices Based on Dense Ceramic Membranes for CO2 Conversion and Utilization, Electrochem. Energy Rev. vol. 4 (2021) 518–544.

[14] R.I. Masel, Z. Liu, H. Yang, J.J. Kaczur, D. Carrillo, S. Ren, D. Salvatore, C. P. Berlinguette, An industrial perspective on catalysts for low-temperature CO2 electrolysis, Nat. Nanotechnol. vol. 16 (2021) 118–128.

[15] T. Burdyny, W.A. Smith, CO2 reduction on gas-diffusion electrodes and why catalytic performance must be assessed at commercially-relevant conditions, Energy Environ. Sci. vol. 12 (5) (2019) 1442–1453.

[16] S.D. Rihm, M.K. Kovalev, A.A. Lapkin, J.W. Ager, M. Kraft, On the role of C 4 and C 5 products in electrochemical CO 2 reduction via copper-based catalysts, Energy Environ. Sci. vol. 16 (2023) 1697–1710.

[17] J.B. Greenblatt, D.J. Miller, J.W. Ager, F.A. Houle, I.D. Sharp, The Technical and Energetic Challenges of Separating (Photo)Electrochemical Carbon Dioxide Reduction Products, Joule vol. 2 (2018) 381–420.

[18] B. Endrődi, E. Kecsenovity, A. Samu, F. Darvas, R.V. Jones, V. Török, A. Danyi, C. Janáky, Multilayer Electrolyzer Stack Converts Carbon Dioxide to Gas Products at High Pressure with High Efficiency, ACS Energy Lett. vol. 4 (2019) 1770–1777.

[19] S. Jin, Z. Hao, K. Zhang, Z. Yan, J. Chen, Advances and Challenges for the Electrochemical Reduction of CO2 to CO: From Fundamentals to Industrialization, Angew. Chem. Int. Ed. vol. 60 (2021) 20627–20648.

[20] A. Isenberg, Energy conversion via solid oxide electrolyte electrochemical cells at high temperatures, Solid State Ion. vol. 3–4 (1981) 431–437.

[21] W. Doenitz, R. Schmidberger, E. Steinheil, R. Streicher, Hydrogen production by high temperature electrolysis of water vapour, Int. J. Hydrog. Energy vol. 5 (1980) 55–63.

[22] W. Doenitz, R. Schmidberger, Concepts and design for scaling up high temperature water vapour electrolysis, Int. J. Hydrog. Energy vol. 7 (1982) 321–330.

[23] W. Dönitz, E. Erdle, High-temperature electrolysis of water vapor—status of development and perspectives for application, Int. J. Hydrog. Energy vol. 10 (1985) 291–295.

[24] W. Dönitz, G. Dietrich, E. Erdle, R. Streicher, Electrochemical high temperature technology for hydrogen production or direct electricity generation, Int. J. Hydrog. Energy vol. 13 (1988) 283–287.

[25] K.R. Sridhar, B.T. Vaniman, Oxygen production on Mars using solid oxide electrolysis, Solid State Ion. vol. 93 (1997) 321–328.

[26] K.R. Sridhar, J.E. Finn, M.H. Kliss, In-situ resource utilization technologies for Mars life support systems, Adv. Space Res. vol. 25 (2000) 249–255.

[27] J. Hartvigsen, S. Elangovan, J. Elwell, D. Larsen, Oxygen production from mars atmosphere carbon dioxide using solid oxide electrolysis, ECS Trans. vol. 78 (2017) 2953–2963.

[28] N. A. S. A MOXIE for Scientists, ⟨https://mars.nasa.gov/mars2020/spacecraft/instruments/moxie/for-scientists/⟩.

[29] M.A. Laguna-Bercero, Recent advances in high temperature electrolysis using solid oxide fuel cells: A review, J. Power Sources vol. 203 (2012) 4–16.

[30] S.D. Ebbesen, S.H. Jensen, A. Hauch, M.B. Mogensen, High Temperature Electrolysis in Alkaline Cells, Solid Proton Conducting Cells, and Solid Oxide Cells, Chem. Rev. vol. 114 (2014) 10697–10734.

[31] J.B. Hansen, Solid oxide electrolysis – a key enabling technology for sustainable energy scenarios, Faraday Discuss. vol. 182 (2015) 9–48.

[32] S.D. Ebbesen, M. Mogensen, Electrolysis of carbon dioxide in Solid Oxide Electrolysis Cells, J. Power Sources vol. 193 (2009) 349–358.

[33] S. Uhm, Y.D. Kim, Electrochemical conversion of carbon dioxide in a solid oxide electrolysis cell, Curr. Appl. Phys. vol. 14 (2014) 672–679.

[34] S. Foit, L. Dittrich, T. Duyster, I. Vinke, R.-A. Eichel, L.G.J. de Haart, Direct Solid Oxide Electrolysis of Carbon Dioxide: Analysis of Performance and Processes, Processes vol. 8 (2020) 1390.

[35] S.D. Ebbesen, C. Graves, M. Mogensen, Production of Synthetic Fuels by Co-Electrolysis of Steam and Carbon Dioxide, Int. J. Green. Energy vol. 6 (2009) 646–660.

[36] Y. Zheng, J. Wang, B. Yu, W. Zhang, J. Chen, J. Qiao, J. Zhang, A review of high temperature co-electrolysis of H2O and CO2to produce sustainable fuels using solid oxide electrolysis cells (SOECs): advanced materials and technology, Chem. Soc. Rev. vol. 46 (2017) 1427–1463.

[37] S.R. Foit, I.C. Vinke, L.G.J. de Haart, R. Eichel, Power-to-Syngas: An Enabling Technology for the Transition of the Energy System? Angew. Chem. Int. Ed. vol. 56 (2017) 5402–5411.

[38] L. Dittrich, M. Nohl, E.E. Jaekel, S. Foit, L.G.J. (Bert) de Haart, R.-A. Eichel, High-Temperature Co-Electrolysis: A Versatile Method to Sustainably Produce Tailored Syngas Compositions, J. Electrochem. Soc. vol. 166 (2019) F971–F975.

[39] R. Küngas, P. Blennow, T. Heiredal-Clausen, T. Holt, J. Rass-Hansen, S. Primdahl, J.B. Hansen, eCOs - A Commercial CO2Electrolysis System Developed by Haldor Topsoe, ECS Trans. vol. 78 (2017) 2879–2884.

[40] R. Snoeckx, A. Bogaerts, Plasma technology – a novel solution for CO2 conversion? Chem. Soc. Rev. vol. 46 (2017) 5805–5863.

[41] A. Hecimovic, F.A. D'Isa, E. Carbone, U. Fantz, Enhancement of CO2 conversion in microwave plasmas using a nozzle in the effluent, J. CO2 Util. vol. 57 (2022) 101870.

[42] A. Hecimovic, C.K. Kiefer, A. Meindl, R. Antunes, U. Fantz, Fast gas quenching of microwave plasma effluent for enhanced CO2 conversion, J. CO2 Util. vol. 71 (2023) 102473.

[43] C.K. Kiefer, R. Antunes, A. Hecimovic, A. Meindl, U. Fantz, CO2 dissociation using a lab-scale microwave plasma torch: An experimental study in view of industrial application, Chem. Eng. J. vol. 481 (2024) 148326.

[44] M. Leins, L. Alberts, M. Kaiser, M. Walker, A. Schulz, U. Schumacher, U. Stroth, Development and Characterisation of a Microwave-heated Atmospheric Plasma Torch, Plasma Process. Polym. vol. 6 (2009).

[45] M. Leins, J. Kopecki, S. Gaiser, A. Schulz, M. Walker, U. Schumacher, U. Stroth, T. Hirth, Microwave Plasmas at Atmospheric Pressure, Contrib. Plasma Phys. vol. 54 (2013) 14–26.

[46] E. Carbone, F. D'Isa, A. Hecimovic, U. Fantz, Analysis of the C2 (d 3 Π g − a 3 Π u) Swan bands as a thermometric probe in CO2 microwave plasmas, Plasma Sources Sci. Technol. vol. 29 (2020) 055003.

[47] A. Herbers, C. Kern, A. Jess, Cobalt Catalyzed Fischer-Tropsch Synthesis with O2-Containing Syngas, Catalysts vol. 13 (2023) 391.

[48] E. Delikonstantis, M. Scapinello, V. Singh, H. Poelman, C. Montesano, L. M. Martini, P. Tosi, G.B. Marin, K.M. Van Geem, V.V. Galvita, G.D. Stefanidis, Exceeding Equilibrium CO2 Conversion by Plasma-Assisted Chemical Looping, ACS Energy Lett. vol. 7 (2022) 1896–1902.

[49] Q. Zheng, Y. Xie, J. Tan, Z. Xu, P. Luo, T. Wang, Z. Liu, F. Liu, K. Zhang, Z. Fang, G. Zhang, W. Jin, Coupling of dielectric barrier discharge plasma with oxygen permeable membrane for highly efficient low-temperature permeation, J. Membr. Sci. vol. 641 (2022) 119896.

[50] F. Buck, K. Wiegers, A. Schulz, T. Schiestel, Effect of plasma atmosphere on the oxygen transport of mixed ionic and electronic conducting hollow fiber membranes, J. Ind. Eng. Chem. vol. 104 (2021) 1–7.

[51] F. Girard-Sahun, O. Biondo, G. Trenchev, G. van Rooij, A. Bogaerts, Carbon bed post-plasma to enhance the CO2 conversion and remove O2 from the product stream, Chem. Eng. J. vol. 442 (2022) 136268.

[52] A. Pandiyan, V. Kyriakou, D. Neagu, S. Welzel, A. Goede, M.C.M. van de Sanden, M.N. Tsampas, CO2 conversion via coupled plasma-electrolysis process, J. CO2 Util. vol. 57 (2022) 101904.

[53] R. Antunes, K. Wiegers, A. Hecimovic, C.K. Kiefer, S. Buchberger, A. Meindl, T. Schiestel, A. Schulz, M. Walker, U. Fantz, Proof of Concept for O2 Removal with Multiple LCCF Membranes Accommodated in the Effluent of a CO2 Plasma Torch, ACS Sustain. Chem. amp; Eng. vol. 11 (2023) 15984–15993.

[54] A. Hecimovic, F. D'Isa, E. Carbone, A. Drenik, U. Fantz, Quantitative gas composition analysis method for a wide pressure range up to atmospheric pressure—CO2 plasma case study, Rev. Sci. Instrum. vol. 91 (2020).

[55] B. Wanten, R. Vertongen, R. De Meyer, A. Bogaerts, Plasma-based CO2 conversion: How to correctly analyze the performance? J. Energy Chem. vol. 86 (2023) 180–196.

[56] S. Deutz, A. Bardow, Life-cycle assessment of an industrial direct air capture process based on temperature–vacuum swing adsorption, Nat. Energy vol. 6 (2021) 203–213.

[57] D.W. Keith, G. Holmes, D.St Angelo, K. Heidel, A Process for Capturing CO2 from the Atmosphere, Joule vol. 2 (2018) 1573–1594.

[58] Muegge website, ⟨www.Muegge.de⟩.

[59] W. Bongers, H. Bouwmeester, B. Wolf, F. Peeters, S. Welzel, D. van den Bekerom, N. den Harder, A. Goede, M. Graswinckel, P.W. Groen, J. Kopecki, M. Leins, G. van Rooij, A. Schulz, M. Walker, R. van de Sanden, Plasma-driven dissociation of CO2 for fuel synthesis, Plasma Process. Polym. vol. 14 (2016).

[60] Industrialmicrowave Website, ⟨www.industrialmicrowave.com⟩.

[61] L. Vialetto, A.W. van de Steeg, P. Viegas, S. Longo, G.J. van Rooij, M.C.M. van de Sanden, J. van Dijk, P. Diomede, Charged particle kinetics and gas heating in CO2 microwave plasma contraction: comparisons of simulations and experiments, Plasma Sources Sci. Technol. vol. 31 (2022) 055005.

[62] R. Hosseini Rad, V. Brüser, M. Schiorlin, J. Schäfer, R. Brandenburg, Enhancement of CO2 splitting in a coaxial dielectric barrier discharge by pressure increase, packed bed and catalyst addition, Chem. Eng. J. vol. 456 (2023) 141072.

[63] Kerogreen website, ⟨www.kerogreen.eu⟩.

[64] DIFFER press release, 16.11.2021, ⟨https://www.differ.nl/news/KEROGREENplasma⟩.

[65] D. Higgins, C. Hahn, C. Xiang, T.F. Jaramillo, A.Z. Weber, Gas-Diffusion Electrodes for Carbon Dioxide Reduction: A New Paradigm, ACS Energy Lett. vol. 4 (2019) 317–324.

[66] K. Ye, G. Zhang, X.-Y. Ma, C. Deng, X. Huang, C. Yuan, G. Meng, W.-B. Cai, K. Jiang, Resolving local reaction environment toward an optimized CO 2 -to-CO conversion performance, Energy Environ. Sci. vol. 15 (2021) 749–759.

[67] S.C. da Cunha, J. Resasco, Maximizing single-pass conversion does not result in practical readiness for CO2 reduction electrolyzers, Nat. Commun. vol. 14 (2023) 5513.

[68] S.A. Hawks, V.M. Ehlinger, T. Moore, E.B. Duoss, V.A. Beck, A.Z. Weber, S. E. Baker, Analyzing Production Rate and Carbon Utilization Trade-offs in CO2RR Electrolyzers, ACS Energy Lett. vol. 7 (2022) 2685–2693.

[69] T. Moore, D.I. Oyarzun, W. Li, T.Y. Lin, M. Goldman, A.A. Wong, S.A. Jaffer, A. Sarkar, S.E. Baker, E.B. Duoss, C. Hahn, Electrolyzer energy dominates separation costs in state-of-the-art CO2 electrolyzers: Implications for single-pass CO2 utilization, Joule vol. 7 (2023) 782–796.

[70] T. Alerte, J.P. Edwards, C.M. Gabardo, C.P. O'Brien, A. Gaona, J. Wicks, A. Obradović, A. Sarkar, S.A. Jaffer, H.L. MacLean, D. Sinton, E.H. Sargent, Downstream of the CO2 Electrolyzer: Assessing the Energy Intensity of Product Separation, ACS Energy Lett. vol. 6 (2021) 4405–4412.

[71] C.M. Gabardo, A. Seifitokaldani, J.P. Edwards, C.-T. Dinh, T. Burdyny, M. G. Kibria, C.P. O'Brien, E.H. Sargent, D. Sinton, Combined high alkalinity and pressurization enable efficient CO 2 electroreduction to CO, Energy Environ. Sci. vol. 11 (2018) 2531–2539.

[72] B.D. Mot, J. Hereijgers, M. Duarte, T. Breugelmans, Influence of flow and pressure distribution inside a gas diffusion electrode on the performance of a flow-by CO2 electrolyzer, Chem. Eng. J. vol. 378 (2019) 122224.

[73] J.P. Edwards, Y. Xu, C.M. Gabardo, C.-T. Dinh, J. Li, Z. Qi, A. Ozden, E.H. Sargent, D. Sinton, Efficient electrocatalytic conversion of carbon dioxide in a low-resistance pressurized alkaline electrolyzer, Appl. Energy vol. 261 (2020) 114305.

[74] J.A. Rabinowitz, M.W. Kanan, The future of low-temperature carbon dioxide electrolysis depends on solving one basic problem, Nat. Commun. vol. 11 (2020) 5231.

[75] M. Ma, E.L. Clark, K.T. Therkildsen, S. Dalsgaard, I. Chorkendorff, B. Seger, Insights into the carbon balance for CO 2 electroreduction on Cu using gas diffusion electrode reactor designs, Energy Environ. Sci. vol. 13 (2020) 977–985.

[76] D. Reinisch, B. Schmid, N. Martić, R. Krause, H. Landes, M. Hanebuth, K.J. J. Mayrhofer, G. Schmid, Various CO2-to-CO Electrolyzer Cell and Operation Mode Designs to avoid CO2-Crossover from Cathode to Anode, Z. F. üR. Phys. Chem. vol. 234 (2019) 1115–1131.

[77] M. Ramdin, O.A. Moultos, L.J.P.V.D. Broeke, P. Gonugunta, P. Taheri, T.J. H. Vlugt, Carbonation in Low-Temperature CO2 Electrolyzers: Causes, Consequences, and Solutions, Ind. Eng. Chem. Res. vol. 62 (2023) 6843–6864.

[78] S. Van Daele, L. Hintjens, S. Hoekx, B. Bohlen, S. Neukermans, N. Daems, J. Hereijgers, T. Breugelmans, How flue gas impurities affect the electrochemical reduction of CO2 to CO and formate, Appl. Catal. B: Environ. vol. 341 (2024) 123345.

[79] W. Luc, B.H. Ko, S. Kattel, S. Li, D. Su, J.G. Chen, F. Jiao, SO2-Induced Selectivity Change in CO2 Electroreduction, J. Am. Chem. Soc. vol. 141 (2019) 9902–9909.

[80] B.H. Ko, B. Hasa, H. Shin, E. Jeng, S. Overa, W. Chen, F. Jiao, The impact of nitrogen oxides on electrochemical carbon dioxide reduction, Nat. Commun. vol. 11 (2020) 5856.

[81] N.J. Harmon, H. Wang, Electrochemical CO2 Reduction in the Presence of Impurities: Influences and Mitigation Strategies, Angew. Chem. Int. Ed. vol. 61 (2022) e202213782.

[82] G. Marcandalli, M.C.O. Monteiro, A. Goyal, M.T.M. Koper, Electrolyte Effects on CO2 Electrochemical Reduction to CO, Acc. Chem. Res. vol. 55 (2022) 1900–1911.

[83] A. Xu, N. Govindarajan, G. Kastlunger, S. Vijay, K. Chan, Theories for Electrolyte Effects in CO2 Electroreduction, Acc. Chem. Res. vol. 55 (2022) 495–503.

[84] B. Endrődi, E. Kecsenovity, A. Samu, T. Halmágyi, S. Rojas-Carbonell, L. Wang, Y. Yan, C. Janáky, High carbonate ion conductance of a robust PiperION membrane allows industrial current density and conversion in a zero-gap carbon dioxide electrolyzer cell, Energy Environ. Sci. vol. 13 (2020) 4098–4105.

[85] S. Garg, C.A.G. Rodriguez, T.E. Rufford, J.R. Varcoe, B. Seger, How membrane characteristics influence the performance of CO 2 and CO electrolysis, Energy Environ. Sci. vol. 15 (2022) 4440–4469.

[86] N. Wang, R.K. Miao, G. Lee, A. Vomiero, D. Sinton, A.H. Ip, H. Liang, E. H. Sargent, Suppressing the liquid product crossover in electrochemical CO2 reduction, SmartMat vol. 2 (2021) 12–16.

[87] A.A. Samu, A. Kormányos, E. Kecsenovity, N. Szilágyi, B. Endrődi, C. Janáky, Intermittent Operation of CO2 Electrolyzers at Industrially Relevant Current Densities, ACS Energy Lett. vol. 7 (2022) 1859–1861.

[88] M. Jouny, W. Luc, F. Jiao, General Techno-Economic Analysis of CO2 Electrolysis Systems, Ind. amp; Eng. Chem. Res. vol. 57 (2018) 2165–2177.

[89] X. Li, P. Anderson, H.-R.M. Jhong, M. Paster, J.F. Stubbins, P.J.A. Kenis, Greenhouse Gas Emissions, Energy Efficiency, and Cost of Synthetic Fuel Production Using Electrochemical CO2 Conversion and the Fischer–Tropsch Process, Energy amp; Fuels vol. 30 (2016) 5980–5989.

[90] M. Quentmeier, B. Schmid, H. Tempel, H. Kungl, R.-A. Eichel, Toward a Stackable CO2-to-CO Electrolyzer Cell Design - Impact of Media Flow Optimization, ACS Sustain. Chem. Eng. vol. 11 (2023) 679–688.

[91] B. Endrődi, A. Samu, E. Kecsenovity, T. Halmágyi, D. Sebők, C. Janáky, Operando cathode activation with alkali metal cations for high current density operation of water-fed zero-gap carbon dioxide electrolysers, Nat. Energy vol. 6 (2021) 439–448.

[92] J.P. Edwards, T. Alerte, C.P. O'Brien, C.M. Gabardo, S. Liu, J. Wicks, A. Gaona, J. Abed, Y.C. Xiao, D. Young, A. Sedighian Rasouli, A. Sarkar, S.A. Jaffer, H. L. MacLean, E.H. Sargent, D. Sinton, Pilot-Scale CO2 Electrolysis Enables a Semi-empirical Electrolyzer Model, ACS Energy Lett. vol. 8 (2023) 2576–2584.

[93] P. Jeanty, C. Scherer, E. Magori, K. Wiesner-Fleischer, O. Hinrichsen, M. Fleischer, Upscaling and continuous operation of electrochemical CO2 to CO conversion in aqueous solutions on silver gas diffusion electrodes, J. CO2 Util. vol. 24 (2018) 454–462.

[94] D. Wakerley, S. Lamaison, J. Wicks, A. Clemens, J. Feaster, D. Corral, S.A. Jaffer, A. Sarkar, M. Fontecave, E.B. Duoss, S. Baker, E.H. Sargent, T.F. Jaramillo, C. Hahn, Gas diffusion electrodes, reactor designs and key metrics of low-temperature CO2 electrolysers, Nat. Energy (2022) 1–14.

[95] G. Gao, C.A. Obasanjo, J. Crane, C.-T. Dinh, Comparative analysis of electrolyzers for electrochemical carbon dioxide conversion, Catal. Today vol. 423 (2023) 114284.

[96] Z. Liu, H. Yang, R. Kutz, R.I. Masel, CO2 Electrolysis to CO and O2 at High Selectivity, Stability and Efficiency Using Sustainion Membranes, J. Electrochem. Soc. vol. 165 (2018) J3371–J3377.

[97] J.J. Kaczur, H. Yang, Z. Liu, S.D. Sajjad, R.I. Masel, Carbon Dioxide and Water Electrolysis Using New Alkaline Stable Anion Membranes, Front. Chem. vol. 6 (2018) 263.

[98] Evonik, ⟨https://www.bmbf.de/bmbf/shareddocs/pressemitteilungen/de/fuer-eine-klimafreundliche-ind-nachhaltige-chemikalien-nutzen.html#searchFacets⟩.

[99] T. Haas, R. Krause, R. Weber, M. Demler, G. Schmid, Technical photosynthesis involving CO2 electrolysis and fermentation, Nat. Catal. vol. 1 (2018) 32–39.

[100] Rheticus project, ⟨https://www.kopernikus-projekte.de/partner-projekte/rheticus⟩.

[101] R. Krause, D. Reinisch, C. Reller, H. Eckert, D. Hartmann, D. Taroata, K. Wiesner-Fleischer, A. Bulan, A. Lueken, G. Schmid, Industrial Application Aspects of the Electrochemical Reduction of CO2 to CO in Aqueous Electrolyte, Chem. Ing. Tech. vol. 92 (2020) 53–61.

[102] S.E. Wolf, F.E. Winterhalder, V. Vibhu, L.G.J. de Haart, O. Guillon, R.-A. Eichel, N.H. Menzler, Solid oxide electrolysis cells – current material development and industrial application, J. Mater. Chem. A vol. 11 (2023) 17977–18028.

[103] TOPSOE, Carbon monoxide - Produce your own carbon monoxide tailored to your business, ⟨https://www.topsoe.com/processes/carbon-monoxide⟩.

[104] ⟨https://www.co2meter.com/blogs/news/co2-purity-grade-charts⟩.

[105] S. Foit, L. Dittrich, M. Nohl, I.C. Vinke, R.-A. Eichel, L.G.J. De Haart, Understanding High-Temperature Electrolysis, ECS Trans. vol. 103 (2021) 487–492.

[106] L. Dittrich, T. Duyster, S. Foit, I.C. Vinke, R.-A. Eichel, L.G.J. (. De Haart, Performance and Processes of Pure CO2 Electrolysis in Solid Oxide Cells, ECS Trans. vol. 103 (2021) 501–509.

[107] F. Thaler, Q. Fang, U. de Haart, L.G.J. (. De Haart, R. Peters, L. Blum, Performance and Stability of Solid Oxide Cell Stacks in CO2-Electrolysis Mode, ECS Trans. vol. 103 (2021) 363–374.

[108] C. Stoots, J. O'Brien, J. Hartvigsen, Results of recent high temperature coelectrolysis studies at the Idaho National Laboratory, Int. J. Hydrog. Energy vol. 34 (2009) 4208–4215.

[109] X. Zhang, Y. Song, G. Wang, X. Bao, Co-electrolysis of CO2 and H2O in high-temperature solid oxide electrolysis cells: Recent advance in cathodes, J. Energy Chem. vol. 26 (2017) 839–853.

[110] S.E. Wolf, L. Dittrich, M. Nohl, T. Duyster, I.C. Vinke, R.-A. Eichel, L.G.J. (Bert) de Haart, Boundary Investigation of High-Temperature Co-Electrolysis Towards Direct CO2 Electrolysis, J. Electrochem. Soc. vol. 169 (2022) 034531.

[111] R. Peters, W. Tiedemann, I. Hoven, R. Deja, N. Kruse, Q. Fang, D. Schäfer, F. Kunz, L. Blum, R. Peters, R.-A. Eichel, Experimental Results of a 10/40 kW-Class Reversible Solid Oxide Cell Demonstration System at Forschungszentrum Jülich, J. Electrochem. Soc. vol. 170 (2023) 044509.

[112] J.C. Mankins, Technology readiness levels, White Pap. (1995).

[113] C.K. Kiefer, R. Antunes, A. Hecimovic, A. Meindl, U. Fantz, CO2 dissociation using a lab-scale microwave plasma torch: an ex-perimental study on industrially relevant parameters, Chemical Engineering Journal 481 (2024) 148326, https://doi.org/10.1016/j.cej.2023.148326.

[114] C. Mittal, C. Hadsbjerg, P. Blennow, Small-scale CO from CO2 using electrolysis, Chem. Eng. World vol. 52 (2017) 44–46.

[115] Topsoe, ⟨https://info.topsoe.com/ecos⟩.

[116] H. Shin, K.U. Hansen, F. Jiao, Techno-economic assessment of low-temperature carbon dioxide electrolysis, Nat. Sustain. vol. 4 (2021) 911–919.

[117] D.H. Shin, S.M. Chun, Y.C. Hong, J.S. Lee, Generation of plasma torch by 2.45 GHz microwaves from a solid-state power amplifier, AIP Adv. vol. 9 (2019).

[118] A.J. Burggraaf, L. Cot, Fundamentals of inorganic membrane science and technology. Fundamentals of Inorganic Membrane Science and Technology, Elsevier, 1996, p. iii.

[119] W.R. Müller E, Materialflüsse der elektrischen undelektronischen Geräte in der Schweiz.